

1 **A global hotspot for dissolved organic carbon in hypermaritime**
2 **watersheds of coastal British Columbia.**

3
4 Allison A. Oliver^{1,2}, Suzanne E. Tank^{1,2}, Ian Giesbrecht^{2,7}, Maartje C. Korver², William C.
5 Floyd^{3,4,2}, Paul Sanborn^{5,2}, Chuck Bulmer⁶, Ken P. Lertzman^{7,2}

6
7 ¹University of Alberta, Department of Biological Sciences, CW 405, Biological Sciences Bldg.,
8 University of Alberta, Edmonton, Alberta, T6G 2E9, Canada

9 ²Hakai Institute, Tula Foundation, Box 309, Heriot Bay, British Columbia, V0P 1H0, Canada

10 ³Ministry of Forests, Lands and Natural Resource Operations, 2100 Labieux Rd, Nanaimo, BC,
11 V9T 6E9, Canada

12 ⁴Vancouver Island University, 900 Fifth Street, Nanaimo, BC, V9R 5S5, Canada

13 ⁵Ecosystem Science and Management Program, University of Northern British Columbia, 3333
14 University Way, Prince George, BC, V2N 4Z9, Canada

15 ⁶BC Ministry of Forests Lands and Natural Resource Operations, 3401 Reservoir Rd, Vernon,
16 BC, V1B 2C7, Canada

17 ⁷School of Resource and Environmental Management, Simon Fraser University, TASC 1- Room
18 8405, 8888 University Drive, Burnaby, BC, V5A 1S6, Canada

19
20 Correspondence to: Allison A. Oliver (aaoliver@ualberta.ca)

21

22

23

24

25

26

27

28

29

30

31

32

33 **Abstract.**

34 The perhumid region of the coastal temperate rainforest (CTR) of Pacific North America
35 is one of the wettest places on Earth and contains numerous small catchments that discharge
36 freshwater and high concentrations of dissolved organic carbon (DOC) directly to the coastal
37 ocean. However, empirical data on the flux and composition of DOC exported from these
38 watersheds is scarce. We established monitoring stations at the outlets of seven catchments on
39 Calvert and Hecate Islands, British Columbia, which represent the rain dominated hypermaritime
40 region of the perhumid CTR. Over several years, we measured stream discharge, stream water
41 DOC concentration, and stream water dissolved organic matter (DOM) composition. Discharge
42 and DOC concentrations were used to calculate DOC fluxes and yields, and DOM composition
43 was characterized using absorbance and fluorescence spectroscopy with parallel factor analysis
44 (PARAFAC). The areal estimate of annual DOC yield in water year 2015 was 33.3 Mg C km⁻²
45 yr⁻¹, with individual watersheds ranging from an average of 24.1-37.7 Mg C km⁻² yr⁻¹. This
46 represents some of the highest DOC yields to be measured at the coastal margin. We observed
47 seasonality in the quantity and composition of exports, with the majority of DOC export
48 occurring during the extended wet period (September-April). Stream flow from catchments
49 reacted quickly to rain inputs, resulting in rapid export of relatively fresh, highly terrestrial-like
50 DOM. DOC concentration and measures of DOM composition were related to stream discharge
51 and stream temperature, and correlated with watershed attributes, including the extent of lakes
52 and wetlands, and thickness of organic and mineral soil horizons. Our discovery of high DOC
53 yields from these small catchments in the CTR is especially compelling as they deliver relatively
54 fresh, highly terrestrial organic matter directly to the coastal ocean. Hypermaritime landscapes
55 are common on the British Columbia coast, suggesting that this coastal margin may play an
56 important role in the regional processing of carbon and in linking terrestrial carbon to marine
57 ecosystems.

58 **1 Introduction**

59 Freshwater aquatic ecosystems process and transport a significant amount of carbon
60 (Cole et al., 2007; Aufdenkampe et al., 2011; Dai et al., 2012). Globally, riverine export is
61 estimated to deliver around 0.9 Pg C yr⁻¹ from land to the coastal ocean (Cole et al., 2007), with
62 typically >50% quantified as dissolved organic carbon (DOC)(Meybeck, 1982; Ludwig et al.,

63 1996; Alvarez-Cobelas et al., 2012; Mayorga et al., 2010). Rivers draining coastal watersheds
64 serve as conduits of DOC from terrestrial and freshwater sources to marine environments
65 (Mulholland and Watts, 1982; Bauer et al., 2013; McClelland et al., 2014) and can have
66 important implications for coastal carbon cycling, biogeochemical interactions, ecosystem
67 productivity, and food webs (Hopkinson et al., 1998; Tallis, 2009; Tank et al., 2012; Regnier et
68 al., 2013). In addition, because the transfer of water and organic matter from watersheds to the
69 coastal ocean represents an important pathway for carbon cycling and ecological subsidies
70 between ecosystems, better understanding of these linkages is needed for constraining
71 predictions of ecosystem productivity in response to perturbations such as climate change. In
72 regions where empirical data are currently scarce, quantifying land-to-ocean DOC export is
73 therefore a priority for improving the accuracy of watershed and coastal carbon models (Bauer et
74 al., 2013).

75 While quantifying DOC flux within and across systems is required for understanding the
76 magnitude of carbon exchange, the composition of DOC (as dissolved organic matter, or DOM)
77 is also important for determining the ecological significance of carbon exported from coastal
78 watersheds. The aquatic DOM pool is a complex mixture that reflects both source material and
79 processing along the watershed terrestrial-aquatic continuum, and as a result can show
80 significant spatial and temporal variation (Hudson et al., 2007; Graeber et al., 2012; Wallin et al.,
81 2015). Both DOC concentration and DOM composition can serve as indicators of watershed
82 characteristics (Koehler et al., 2009), hydrologic flow paths (Johnson et al., 2011; Helton et al.,
83 2015), and watershed biogeochemical processes (Emili and Price, 2013). DOM composition can
84 also influence its role in downstream processing and ecological function, such as susceptibility to
85 biological (Judd et al., 2006) and physiochemical interactions (Yamashita and Jaffé, 2008).

86 The coastal temperate rainforests (CTR) of Pacific North America extend from the Gulf
87 of Alaska, through British Columbia, to Northern California and span a wide range of
88 precipitation and climate regimes. Within this rainforest region, the “perhumid” zone has cool
89 summers and summer precipitation is common (>10% of annual precipitation) (Alaback,
90 1996)(Fig. 1). The perhumid CTR extends from southeast Alaska through the outer coast of
91 central British Columbia and contains forests and soils that have accumulated large amounts of
92 organic carbon above and below ground (Leighty et al., 2006; Gorham et al., 2012). Due to high

93 amounts of precipitation and close proximity to the coast, this area represents a potential hotspot
94 for the transport and metabolism of carbon across the land-to-ocean continuum, and quantifying
95 these fluxes is pertinent for understanding global carbon cycling.

96 Within the large perhumid CTR, there is substantial spatial variation in climate and
97 landscape characteristics that create uncertainty about carbon cycling and pattern. In Alaska, for
98 example, riverine DOC concentrations vary with wetland cover (D'Amore et al. 2015a) and
99 glacial cover (Fellman et al. 2014). Previous studies have shown that streams in southeast Alaska
100 can contain high DOC concentrations (Fellman et al., 2009a; D'Amore et al., 2015a) and
101 produce high DOC yields (D'Amore et al., 2015b; D'Amore et al., 2016, Stackpoole et al.,
102 2016), but no known field estimates have been generated for the perhumid CTR of British
103 Columbia, an area of approximately 97,824 km² (adapted from Wolf et al., 1995). Within the
104 perhumid CTR of British Columbia, terrestrial ecologists have defined a large (29,935 km²)
105 *hypermaritime* sub-region where rainfall dominates over snow, seasonality is moderated by the
106 ocean, and wetlands are extensive (Pojar et al., 1991; area estimated using British Columbia
107 Biogeoclimatic Ecosystem Classification Subzone/Variant mapping Version 10, August 31,
108 2016, available at: [https://catalogue.data.gov.bc.ca/dataset/f358a53b-ffde-4830-a325-](https://catalogue.data.gov.bc.ca/dataset/f358a53b-ffde-4830-a325-a5a03ff672c3)
109 [a5a03ff672c3](https://catalogue.data.gov.bc.ca/dataset/f358a53b-ffde-4830-a325-a5a03ff672c3)). Previous work in the hypermaritime CTR showed that DOC concentrations are
110 high in small streams and tend to increase during rain events (Gibson et al., 2000; Fitzgerald et
111 al., 2003; Emili and Price, 2013). Taken together, these conditions should be expected to
112 generate high yields and fluxes of DOC from hypermaritime watersheds to the coastal ocean.

113 The objectives of this study were to provide the first field-based estimates of DOC
114 exports from watersheds in the extensive hypermaritime region of British Columbia's perhumid
115 CTR, to describe the temporal and spatial dynamics of exported DOC concentration and DOM
116 composition, and to identify relationships between DOC concentration, DOM composition, and
117 watershed characteristics.

118 **2 Methods**

119 **2.1 Study Sites**

120 Study sites are located on northern Calvert Island and adjacent Hecate Island on the
121 central coast of British Columbia, Canada (Lat 51.650, Long -128.035; Fig. 1). Average annual
122 precipitation and air temperature at sea level from 1981-2010 was 3356 mm yr⁻¹ and 8.4 °C

123 (average annual min= 0.9°C, average annual max= 17.9°C) (available online at
124 <http://www.climatewna.com/>; Wang et al., 2012), with precipitation dominated by rain, and
125 winter snowpack persisting only at higher elevations. Sites are located within the hypermaritime
126 region of the CTR on the outer coast of British Columbia. Soils overlying the granodiorite
127 bedrock (Roddick, 1996) are usually < 1 m thick, and have formed in sandy colluvium and
128 patchy morainal deposits, with limited areas of coarse glacial outwash. Chemical weathering and
129 organic matter accumulation in the cool, moist climate have produced soils dominated by
130 Podzols and Follic Histosols, with Hemists up to 2 m thick in depressional sites (IUSS Working
131 Group WRB, 2015). The landscape is comprised of a mosaic of ecosystem types, including
132 exposed bedrock, extensive wetlands, bog forests and woodlands, with organic rich soils (Green,
133 2014; Thompson et al., 2016). Forest stands are generally short with open canopies reflecting the
134 lower productivity of the hypermaritime forests compared to the rest of the perhumid CTR
135 (Banner et al., 2005). Dominant trees are western redcedar, yellow-cedar, shore pine and western
136 hemlock with composition varying across topographic and edaphic gradients. Widespread
137 understory plants include bryophytes, salal, deer fern, and tufted clubrush. Wetland plants are
138 locally abundant including diverse *Sphagnum* mosses and sedges. Although the watersheds have
139 no history of mining or industrial logging, archaeological evidence suggests that humans have
140 occupied this landscape for at least 13,000 years (McLaren et al., 2014). This occupation has had
141 a local effect on forest productivity near habitation sites (Trant et al., 2016) and on fire regimes
142 (Hoffman et al., 2016). We selected seven watersheds with streams draining directly into the
143 ocean (Fig. 1). These numbered watersheds (626, 693, 703, 708, 819 844, and 1015) range in
144 size (3.2 to 12.8 km²) and topography (maximum elevation 160 m to 1012 m), are variably
145 affected by lakes (0.3 – 9.1% lake coverage), and – as is characteristic of the perhumid CTR–
146 have a high degree of wetland coverage (24– 50%) (Table 1).

147 **2.2 Soils and watershed characteristics**

148 Watersheds and streams were delineated using a 3 m resolution digital elevation model
149 (DEM) derived from airborne laser scanning (LiDAR) and flow accumulation analysis using
150 geographic information systems (GIS) to summarize watershed characteristics for each
151 watershed polygon and for all watersheds combined (Gonzalez Arriola et al., 2015; Table 1).
152 Topographic measures were estimated from the DEM, and lake and wetland cover estimated

153 from Province of British Columbia Terrestrial Ecosystem Mapping (TEM) (Green, 2014), and
154 soil material thickness estimated from unpublished digital soil maps (Supplemental S1). We
155 recorded thickness of organic soil material, thickness of mineral soil material, and total soil depth
156 to bedrock at a total of 353 field sites. Mineral soil horizons have $\leq 17\%$ organic C, while
157 organic soil horizons have $> 17\%$ organic C, per the Canadian System of Soil Classification (Soil
158 Classification Working Group, 1998). In addition to field-sampled sites, 40 sites with exposed
159 bedrock (0 cm soil depth) were located using aerial photography. Soil thicknesses were
160 combined with a suite of topographic, vegetation, and remote sensing (LiDAR and RapidEye
161 satellite imagery) data for each sampling point and used to train a random forest model
162 (randomForest package in R; Liaw and Wiener, 2002) that was used to predict soil depth values.
163 Soil material thicknesses were then averaged for each watershed (Table 1). For additional details
164 on field site selection and methods used for predictions of soil thickness, see Supplemental S1.1.

165 **2.3 Sample Collection and Analysis**

166 From May 2013 to July 2016, we collected stream water grab samples from each
167 watershed stream outlet every 2-3 weeks ($n_{\text{total}}= 402$), with less frequent sampling (\sim monthly)
168 during winter (Fig. 1). All samples were filtered in the field (Millipore Millex-HP Hydrophilic
169 PES 0.45 μm) and kept in the dark, on ice until analysis. DOC samples were filtered into 60 mL
170 amber glass bottles and preserved with 7.5M H_3PO_4 . Fe samples were filtered into 125 mL
171 HDPE bottles and preserved with 8M HNO_3 . DOC and Fe samples were analyzed at the BC
172 Ministry of the Environment Technical Services Laboratory (Victoria, BC, Canada). DOC
173 concentrations were determined on a TOC analyzer (Aurora 1030; OI-Analytical) using wet
174 chemical oxidation with persulfate followed by infrared detection of CO_2 . Fe concentrations
175 were determined on a dual-view ICP-OES spectrophotometer (Prodigy; Teledyne Leeman Labs)
176 using a Seaspray pneumatic nebulizer.

177 In May 2014, we began collecting stream samples for stable isotopic composition of $\delta^{13}\text{C}$
178 in DOC ($\delta^{13}\text{C}$ -DOC; $n= 173$) and optical characterization of DOM using absorbance
179 spectroscopy ($n= 259$). Beginning in January 2016, we also analyzed samples using fluorescence
180 spectroscopy (see section 2.6). Samples collected for $\delta^{13}\text{C}$ -DOC were filtered into 40 mL EPA
181 glass vials and preserved with H_3PO_4 . $\delta^{13}\text{C}$ -DOC samples were analyzed at GG Hatch Stable
182 Isotope Laboratory (Ottawa, ON, Canada) using high temperature combustion (TIC-TOC

183 Combustion Analyser Model 1030; OI Analytical) coupled to a continuous flow isotope ratio
184 mass spectrometry (Finnigan Mat DeltaPlusXP; Thermo Fischer Scientific)(Lalonde et al. 2014).
185 Samples analyzed for optical characterization using absorbance and fluorescence were filtered
186 into 125 mL amber HDPE bottles and analyzed at the Hakai Institute (Calvert Island, BC,
187 Canada) within 24 hours of collection.

188 **2.4 Hydrology: Precipitation and Stream Discharge**

189 We measured precipitation using a TB4-L tipping bucket rain gauge with a 0.2 mm
190 resolution (Campbell Scientific Ltd.) located in watershed 708 (elevation= 16 m a.s.l). The rain
191 gauge was calibrated twice per year using a Field Calibration Device, model 653 (HYQUEST
192 Solutions Ltd).

193 We determined continuous stream discharge for each watershed by developing stage
194 discharge rating curves at fixed hydrometric stations situated in close proximity to each stream
195 outlet. Sites were located above tidewater influence and were selected based on favourable
196 conditions (i.e., channel stability and stable hydraulic conditions) for the installation and
197 operation of pressure transducers to measure stream stage. From August 2014 to May 2016 (21
198 months), we measured stage every 5 minutes using an OTT PLS –L (OTT Hydromet, Colorado,
199 USA) pressure transducer (0-4 m range SDI-12) connected to a CR1000 (Campbell Scientific,
200 Edmonton, Canada) data logger. Stream discharge was measured over various intervals using
201 either the velocity area method (for flows $< 0.5 \text{ m}^3\text{s}^{-1}$; ISO Standard 9196:1992, ISO Standard
202 748:2007) or salt dilution (for flows $> 0.5 \text{ m}^3\text{s}^{-1}$; Moore, 2005). Rating curves were developed
203 using the relationship between stream stage height and stream discharge (Supplemental S2).

204 **2.5 DOC flux**

205 From October 1, 2014 to April 30, 2016, we estimated DOC flux for each watershed
206 using measured DOC concentrations (n= 224) and continuous discharge recorded at 15-minute
207 intervals. The watersheds in this region respond rapidly to rain inputs and as a result DOC
208 concentrations are highly variable. To address this variability, routine DOC concentration data
209 (as described in section 2.2) were supplemented with additional grab samples (n= 21) collected
210 around the peak of the hydrograph during several high flow events throughout the year. We
211 performed watershed-specific estimates of DOC flux using the “rloadest” package (Lorenz et al.,
212 2015) in R (version 3.2.5, R Core Team, 2016), which replicates functions developed in the U.S.

213 Geological Survey load-estimator program, LOADEST (Runkel et al., 2004). LOADEST is a
214 multiple-regression adjusted maximum likelihood estimation model that calibrates a regression
215 between measured constituent values and stream flow across seasons and time and then fits it to
216 combinations of coefficients representing nine predetermined models of constituent flux. To
217 account for potentially small sample size, the best model was selected using the second order
218 Akaike Information Criterion (AICc) (Akaike, 1981; Hurvich and Tsai, 1989). Input data were
219 log-transformed to avoid bias and centered to reduce multicollinearity. For additional details on
220 model selection, see Supplemental Table S3.1.

221 **2.6 Optical characterization of DOM**

222 Prior to May 2014, absorbance measures of water samples (n= 99) were conducted on a
223 Varian Cary-50 (Varian, Inc.) spectrophotometer at the BC Ministry of the Environment
224 Technical Services Laboratory (Victoria, BC, Canada) to determine specific UV absorption at
225 254 nm (SUVA₂₅₄). After May 2014, we conducted optical characterization of DOM by
226 absorbance and fluorescence spectroscopy at the Hakai Institute field station (Calvert Island, BC,
227 Canada) using an Aqualog fluorometer (Horiba Scientific, Edison, New Jersey, USA). Strongly
228 absorbing samples (absorbance units > 0.2 at 250 nm) were diluted prior to analysis to avoid
229 excessive inner filter effects (Lakowicz, 1999). Samples were run in 1 cm quartz cells and
230 scanned from 220-800 nm at 2 nm intervals to determine SUVA₂₅₄ as well as the spectral slope
231 ratio (S_R). SUVA₂₅₄ has been shown to positively correlate with increasing molecular aromaticity
232 associated with the fulvic acid fraction of DOM (Weishaar et al., 2003), and is calculated by
233 dividing the Decadic absorption coefficient at 254 nm by DOC concentration (mg C L⁻¹). To
234 account for potential Fe interference with absorbance values, we corrected SUVA₂₅₄ values by Fe
235 concentration according the method described in Poulin et al., (2014). S_R has been shown to
236 negatively correlate with molecular weight (Helms et al., 2008), and is calculated as the ratio of
237 the spectral slope from 275 nm to 295 nm ($S_{275-295}$) to the spectral slope from 350 nm to 400 nm
238 ($S_{350-400}$).

239 We measured excitation and emission spectra (as excitation emission matrices, EEMs) on
240 samples every three weeks from January to July 2016 (n= 63). Samples were run in 1 cm quartz
241 cells and scanned from excitation wavelengths of 230-550 nm at 5nm increments, and emission
242 wavelengths of 210-620 nm at 2 nm increments. The Horiba Aqualog applied the appropriate

243 instrument corrections for excitation and emission, inner filter effects, and Raman signal
244 calibration. We calculated the Fluorescence Index and Freshness Index for each EEM. The
245 Fluorescence Index is often used to indicate DOM source, where higher values are more
246 indicative of microbial-derived sources of DOM and lower values indicate more terrestrial-
247 derived sources (McKnight et al., 2001), and is calculated as the ratio of emission intensity at
248 450 nm to 500 nm, at an excitation of 370 nm. The Freshness Index is used to indicate the
249 contribution of autochthonous or recently microbial-produced DOM, with higher values
250 suggesting greater autochthony (i.e., microbial inputs), and is calculated as the ratio of emission
251 intensity at 380 nm to the maximum emission intensity between 420 nm and 435 nm, at
252 excitation 310 nm (Wilson and Xenopoulos, 2009).

253 To further characterize features of DOM composition, we performed parallel factor
254 analysis (PARAFAC) using EEM data within the drEEM toolbox for Matlab (Mathworks, MA,
255 USA) (Murphy et al., 2013). PARAFAC is a statistical technique used to decompose the
256 complex mixture of the fluorescing DOM pool into quantifiable, individual components
257 (Stedmon et al., 2003). We detected a total of six unique components, and validated the model
258 using core consistency and split-half analysis (Murphy et al., 2013; Stedmon and Bro, 2008).
259 Components with similar spectra from previous studies were identified using the online
260 fluorescence repository, OpenFluor (Murphy et al., 2014), and additional components with
261 similar peaks were identified through literature review. Since the actual chemical structure of
262 fluorophores is unknown, we used the concentration of each fluorophore as maximum
263 fluorescence of excitation and emission in Raman Units (F_{\max}) to derive the percent contribution
264 of each fluorophore component to total fluorescence. Relationships between PARAFAC
265 components were also evaluated using Pearson correlation coefficients in the R package “Hmisc”
266 (Harrell et al., 2016).

267 **2.7 Evaluating relationships in DOC concentration and DOM composition with stream** 268 **discharge and temperature**

269 We used linear mixed effects models to assess the relationship between DOC
270 concentration or DOM composition ($\delta^{13}\text{C}$ -DOC, S_R , SUVA_{254} , Fluorescence Index, Freshness
271 Index, PARAFAC components), stream discharge, and stream temperature. Analysis was
272 performed in R using the nlme package (Pinheiro et al., 2016). Watershed was included as a

273 random intercept to account for repeat measures on each watershed. For some parameters, a
274 random slope of either discharge or temperature was also included based on data assessment and
275 model selection. Model selection was performed using AIC to compare models fit using
276 Maximum Likelihood (ML) (Burnham and Anderson, 2002; Symonds and Moussalli, 2010). The
277 final model was fit using Restricted Maximum Likelihood (REML). Marginal R^2 , which
278 represents an approximation of the proportion of the variance explained by the fixed factors
279 alone, and conditional R^2 , which represents an approximation of the proportion of the variance
280 explained by both the fixed and random factors, were calculated based on the methods described
281 in Nakagawa and Schielzeth (2013) and Johnson (2014).

282 **2.8 Redundancy analysis: Relationships between DOC concentration, DOM composition,** 283 **and watershed characteristics**

284 We evaluated relationships between stream water DOC and watershed characteristics by
285 relating DOC concentration and measures of DOM composition to catchment attributes using
286 redundancy analysis (RDA; type 2 scaling) in the package rdaTest (Legendre and Durand, 2014)
287 in R (version 3.2.2, R Core Team, 2015). To maximize the amount of information available, we
288 performed RDA analysis on samples collected from January to July 2016, and therefore included
289 all parameters of optical characterization (i.e., all PARAFAC components and spectral indices).
290 We assessed the collinearity of DOM compositional variables using a variance inflation factor
291 (VIF) criteria of > 10 , which resulted in the removal of PARAFAC components C2, C3, and C5
292 prior to RDA analysis. Catchment attributes for each watershed included average slope, percent
293 area of lakes, percent area of wetlands, average depth of mineral soil, and average depth of
294 organic soil. Relationships between variables were linear, so no transformations were necessary
295 and variables were standardized prior to analysis. To account for repeat monthly measures per
296 watershed and potential temporal correlation associated with monthly sampling, we included
297 sample month as a covariable (“partial-RDA”). To test whether the RDA axes significantly
298 explained variation in the dataset, we compared permutations of residuals using ANOVA (9,999
299 iterations; test.axes function of rdaTest).

300 **3 Results**

301 **3.1 Hydrology**

302 We present work for water year 2015 (WY2015; October 1, 2014 – September 30, 2015)
303 and water year 2016 (WY2016; October 1, 2015 – September, 30, 2016). Annual precipitation
304 for both water years was lower than historical mean annual precipitation (WY2015= 2661 mm;
305 WY2016= 2587 mm). It is worth noting that mean annual precipitation at our rain gauge location
306 (2890 mm yr⁻¹, elevation = 16 m) is substantially lower than the average amount received at
307 higher elevations, which from 1981-2010 was approximately 5027 mm yr⁻¹ at an elevation of
308 1000m within our study area. This area receives a very high amount of annual rainfall but also
309 experiences seasonal variation, with an extended wet period from fall through spring, and a much
310 shorter, typically drier period during summer. In WY2015 and WY2016, 86-88% of the annual
311 precipitation on Calvert Island occurred during the 8-months of wetter and cooler weather
312 between September and April (~ 75% of the year), designated the “wet period” (WY2015 wet=
313 2388 mm, average air temp= 7.97°C; WY2016 wet= 2235 mm; average air temp= 7.38°C). The
314 remaining annual precipitation occurred during the drier and warmer summer months of May –
315 August, designated the “dry period” (WY2015 dry= 314 mm, average air temp= 13.4°C;
316 WY2016 dry= 352 mm, average air temp= 13.1°C). Overall, although WY2015 was slightly
317 wetter than WY2016, the two years were comparable in relative precipitation during the wet
318 versus dry periods.

319 Stream discharge (Q) responded rapidly to rain events and as a result, closely tracked
320 patterns in total precipitation (Fig. 2). Total Q for all watersheds was on average 22% greater for
321 the wet period of WY2015 (total Q= 223.02 * 10⁶; range= 5.13 * 10⁶ – 111.51 * 10⁶ m³)
322 compared to the wet period of WY2016 (total Q= 182.89 * 10⁶; range= 4.17 * 10⁶ – 91.45 * 10⁶
323 m³). Stream discharge and stream temperature were significantly different for wet versus dry
324 periods (Mann-Whitney tests, p< 0.0001).

325 **3.2 Temporal and spatial patterns in DOC concentration, yield and flux**

326 Stream waters were high in DOC concentration relative to the global average for
327 freshwater discharged directly to the ocean (average DOC for Calvert and Hecate Islands = 10.4
328 mg L⁻¹, std= 3.8; average global DOC= ~ 6 mg L⁻¹) (Meybeck, 1982; Harrison et al., 2005)
329 (Table 1; Fig. 3). Q-weighted average DOC concentrations were higher than average measured
330 DOC concentrations (11.1 mg L⁻¹, Table 1), and also resulted in slightly different ranking of the
331 watersheds for highest to lowest DOC concentration. Within watersheds, Q-weighted DOC

332 concentrations ranged from a low of 8.4 mg L⁻¹ (watershed 693) to a high of 19.3 mg L⁻¹
333 (watershed 819), and concentrations were significantly different between watersheds (Kruskal-
334 Wallis test, $p < 0.0001$). Seasonal variability tended to be higher in watersheds where DOC
335 concentration was also high (watersheds 626, 819, and 844) and lower in watersheds with greater
336 lake area (watersheds 1015 and 708) (Table 1; box plots, Figure 3). On an annual basis, DOC
337 concentrations generally decreased through the wet period, and increased through the dry period,
338 and concentrations were significantly lower during the wet period compared to the dry period
339 (Mann-Whitney test, $p = 0.0123$). Results of our linear mixed effects (LME) model
340 (Supplemental Table S6.1) indicate that DOC concentration was positively related to both
341 discharge ($b = 0.613$, $p < 0.001$) and temperature ($b = 0.162$, $p = 0.011$) (model conditional $R^2 =$
342 0.57 , marginal $R^2 = 0.09$).

343 Annual and monthly DOC yields are presented in Table 1. For the total period of
344 available Q (October 1, 2014 - April 30, 2016; 19 months), areal (all watersheds) DOC yield was
345 52.3 Mg C km⁻² (95% CI= 45.7 to 68.2 Mg C km⁻²) and individual watershed yields ranged from
346 24.1 to 43.6 Mg C km⁻². For WY2015, areal annual DOC yield was 33.3 Mg C km⁻² yr⁻¹ (95%
347 CI= 28.9 to 38.1 Mg C km⁻² yr⁻¹). Total monthly rainfall was strongly correlated with monthly
348 DOC yield (Fig. 4), and average monthly yield for the wet period (3.35 Mg C km⁻² mo⁻¹; 95%
349 CI= 2.94 to 4.40 Mg C km⁻² mo⁻¹) was significantly greater than average monthly yield during
350 the dry period (0.50 Mg C km⁻² mo⁻¹; 95% CI= 0.41 to 0.62 Mg C km⁻² mo⁻¹) (Mann-Whitney
351 test, $p < 0.0001$).

352 Across our study watersheds, DOC flux generally increased with increasing watershed
353 area (Fig. 5). In WY2015, total DOC flux for all watersheds included in our study was 1562 Mg
354 C (95% CI= 1355 to 1787 Mg C), and individual watershed flux ranged from 82 to
355 276 Mg C. DOC flux was significantly different in wet versus dry periods (Mann-Whitney test, p
356 < 0.0001). Overall, 94% of the export in WY2015 occurred during the wet period, and export for
357 the wet period of WY2015 was lower than export for the wet period of WY2016 (Fig. 5).

358 **3.3 Temporal and spatial patterns in DOM composition**

359 The stable isotopic composition of dissolved organic carbon ($\delta^{13}\text{C-DOC}$) was relatively
360 tightly constrained over space and time (average $\delta^{13}\text{C-DOC} = -26.53\text{‰}$, std= 0.36; range= -
361 27.67‰ to -24.89‰). Values of S_R were low compared to the range typically observed in surface

362 waters (average $S_R = 0.78$, std= 0.04; range= 0.71 to 0.89) and Fe-corrected SUVA₂₅₄ values
363 were at the high end of the range compared to most surface waters (average SUVA₂₅₄ for Calvert
364 and Hecate Islands= 4.42 L mg⁻¹ m⁻¹, std= 0.46; range of SUVA₂₅₄ in surface waters = 1.0 to 5.0
365 L mg⁻¹ m⁻¹) (Spencer et al., 2012). Values for both Fluorescence Index (average Fluorescence
366 Index= 1.36, std= 0.04; range= 1.30 to 1.44) and Freshness Index (average Freshness Index=
367 0.46, std= 0.02; range= 0.41 to 0.49) were relatively low compared to the typical range found in
368 surface waters (Fellman et al., 2010; Hansen et al., 2016). Differences between watersheds were
369 observed for $\delta^{13}\text{C}$ -DOC (Kruskal-Wallis test, $p= 0.0043$), S_R (Kruskal-Wallis test, $p= 0.0001$),
370 Fluorescence Index (Kruskal-Wallis test, $p= 0.0030$), and Freshness Index (Kruskal-Wallis test,
371 $p= 0.0099$), but watersheds did not differ in SUVA₂₅₄ (Kruskal-Wallis test, $p= 0.4837$).

372 We observed seasonal variability in $\delta^{13}\text{C}$ -DOC throughout the period of sample (Fig. 3
373 and our LME model (Supplemental Table S6.1) indicate that $\delta^{13}\text{C}$ -DOC declined with increasing
374 discharge ($b= -0.049$, $p= 0.014$) and stream temperature ($b= -0.024$, $p< 0.001$) (model
375 conditional $R^2= 0.35$, marginal $R^2= 0.10$). In contrast, although SUVA₂₅₄ appeared to exhibit a
376 general seasonal trend of values increasing over the wet period and decreasing over the dry
377 period, SUVA₂₅₄ was not significantly related to either discharge or stream temperature in the
378 LME model results. S_R also appeared to fluctuate seasonally, with lower values during the wet
379 season and higher values during the dry season. S_R was negatively related to discharge ($b= -$
380 0.026 , $p< 0.001$) and positively related to the interaction between discharge and stream
381 temperature ($b= 0.0015$, $p< 0.001$) (model conditional $R^2= 0.62$, marginal $R^2= 0.28$). Freshness
382 Index was negatively related to stream temperature ($b= -0.003$, $p= 0.008$) (model conditional $R^2=$
383 0.59 , marginal $R^2= 0.23$), while Fluorescence Index was not significantly related to either
384 discharge or stream temperature.

385 **3.4 PARAFAC characterization of DOM**

386 Six fluorescence components were identified through PARAFAC (“C1” through “C6”)
387 (Table 2). Additional details on PARAFAC model results are provided in Supplemental Table
388 S4.1, Fig. S4.2, and Fig. S4.3. Of the six components, four were found to have close spectral
389 matches in the OpenFluor database (C1, C3, C5, C6; minimum similarity score > 0.95), while
390 the remaining two (C2 and C4) were found to have similar peaks represented in the literature.
391 The first four components (C1 through C4) are described as terrestrial-derived, whereas

392 components C5 and C6 are described as autochthonous or microbially-derived (Table 2). In
393 general, the rank order of each components' percent contribution to total fluorescence was
394 maintained over time, with C1 comprising the majority of total fluorescence across all
395 watersheds (Fig. 6).

396 Across watersheds, components fluctuated synchronously over time and variation
397 between watersheds was relatively low, although slightly more variation between watersheds
398 was observed during the beginning of the dry period relative to other times of the year (Fig 6).
399 The percent contributions of components C1, C3, C5 and C6 to total fluorescence were not
400 significantly different across watersheds (for all components Kruskal-Wallis test, $p > 0.05$),
401 however percent composition of both C2 and C4 were different (Kruskal-Wallis test, $p = 0.0306$
402 and $p = 0.0307$, respectively) and higher for watersheds 819 and 844 relative to the other
403 watersheds (Supplemental Fig. S4.4).

404 PARAFAC components exhibited significant relationships with stream discharge and
405 stream temperature, although predicted changes (beta, or b) in fluorescence components with
406 discharge and/or stream temperature were small (Supplemental Table S6.2). C3 increased with
407 discharge ($b = 0.006$, $p = 0.003$), whereas C2, C4, and C5 decreased with discharge (C2: $b = -$
408 0.005 , $p = 0.022$; C4: $b = -0.008$, $p = 0.002$; C5: $b = -0.008$, $p = 0.002$). C1, C4, and C6 increased
409 with temperature (C1: $b = 0.001$, $p = 0.050$; C4: $b = 0.003$, $p < 0.001$; C6: $b = 0.005$, $p = 0.005$),
410 while both C3 and C5 decreased with temperature (C3: $b = -0.003$, $p = 0.003$; C5: $b = -0.003$, $p =$
411 0.027). Conditional R^2 values for the models ranged from 0.28 to 0.69, while marginal R^2 ranged
412 from 0.20 to 0.46. Overall, greater changes in component contribution to total fluorescence were
413 observed with changes in discharge relative to changes in stream temperature.

414 **3.5 Relationships between watershed characteristics, DOC concentrations, and DOM** 415 **composition**

416 Results of the partial-RDA (type 2 scaling) were significant in explaining variability in
417 DOM concentration and composition (semi-partial $R^2 = 0.33$, $F = 7.90$, $p < 0.0001$) (Fig. 7). Axes
418 1 through 3 were statistically significant at $p < 0.001$, and the relative contribution of each axis to
419 the total explained variance was 47%, 30%, and 22%, respectively. Additional details on the
420 RDA test are provided in Supplemental Figs. S5.1-S5.2 and Tables S5.3 – S5.5. Axis 1 described
421 a gradient of watershed coverage by water-inundated ecosystem types, ranging from more

422 wetland coverage to more lake coverage. Total lake coverage (area) and mean mineral soil
423 material thickness showed a strong positive contribution, and wetland coverage (area) showed a
424 strong negative contribution to this axis. Freshness Index, Fluorescence Index, S_R and
425 fluorescence component C6 were positively correlated with Axis 1, while component C4 showed
426 a clear negative correlation. Axis 2 described a subtler gradient of soil material thickness ranging
427 from greater mean organic soil material thickness to greater mean mineral soil material
428 thickness. DOC concentration, $\delta^{13}\text{C}$ -DOC, SUVA_{254} , and fluorescence component C1 all showed
429 a strong, positive correlation with Axis 2. Axis 3 described a gradient of watershed steepness,
430 from lower gradient slopes with more wetland area and thicker organic soil material to steeper
431 slopes with less developed organic horizons. Average slope contributed negatively to Axis 3 (see
432 Supplemental Table S5.5), followed by positive contributions from both wetland area and
433 thickness of organic soil material. $\delta^{13}\text{C}$ -DOC showed the most positive correlation with Axis 3,
434 whereas fluorescence components C1 and C4 showed the most negative.

435 **4 Discussion**

436 **4.1 DOC export from small catchments to the coastal ocean**

437 In comparison to global models of DOC export (Mayorga et al., 2010) and DOC exports
438 quantified for southeastern Alaska (D'Amore et al., 2015a; D'Amore et al., 2016; Stackpoole et
439 al., 2017), our estimates of freshwater DOC yield from Calvert and Hecate Island watersheds are
440 in the upper range predicted for the perhumid rainforest region. When compared to watersheds of
441 similar size, DOC yields from Calvert and Hecate Island watersheds are some of the highest
442 observed (see reviews in Hope et al., 1994; Alvarez-Cobelas et al., 2012), including DOC yields
443 from many tropical rivers, despite the fact that tropical rivers have been shown to export very
444 high DOC (e.g., Autuna River, Venezuela, DOC yield= 56,946 kg C km⁻² yr⁻¹; Castillo et al.,
445 2004), and are often regarded as having disproportionately high carbon export compared to
446 temperate and Arctic rivers (Aitkenhead and McDowell, 2000; Borges et al., 2015). Our
447 estimates of DOC yield are comparable to, or higher than, previous estimates from high-latitude
448 catchments of similar size that receive high amounts of precipitation and contain extensive
449 organic soils and wetlands (e.g. Naiman, 1982 (DOC yield= 48,380 kg C km⁻² yr⁻¹); Brooks et
450 al., 1999 (DOC yield= 20,300 kg C km⁻² yr⁻¹); Ågren et al., 2007 (DOC yield= 32,043 kg C km⁻²
451 yr⁻¹)). However, many of these catchments represent low (first or second) order headwater

452 streams that drain to higher order stream reaches, rather than directly to the ocean. Although
453 headwater streams have been shown to export up to 90% of the total annual carbon in stream
454 systems (Leach et al., 2016), significant processing and loss typically occurs during downstream
455 transit (Battin et al., 2008).

456 Over much of the incised outer coast of the CTR, small rainfall-dominated catchments
457 contribute high amounts of freshwater runoff to the coastal ocean (Royer, 1982; Morrison et al.,
458 2012; Carmack et al., 2015). Small mountainous watersheds that discharge directly to the ocean
459 can exhibit disproportionately high fluxes of carbon relative to watershed size, and in aggregate
460 may deliver more than 50% of total carbon flux from terrestrial systems to the ocean (Milliman
461 and Syvitski, 1992; Masiello and Druffel, 2001). Extrapolating our estimate of annual DOC yield
462 from Calvert and Hecate Island watersheds to the entire hypermaritime subregion of British
463 Columbia's CTR (29,935 km²), generates an estimated annual DOC flux of 0.997 Tg C yr⁻¹
464 (0.721 to 1.305 Tg C yr⁻¹ for our lowest to highest yielding watersheds, respectively), with the
465 caveat that this estimate is rudimentary and does not account for spatial heterogeneity in
466 controlling factors such as wetland extent, topography, and watershed size. Regional
467 comparisons estimate that Southeast Alaska (104,000 km²), at the northern range of the CTR,
468 exports approximately 1.25 Tg C yr⁻¹ (Stackpoole et al., 2016), while south of the perhumid
469 CTR, the wet northwestern United States and its associated coastal temperate rainforests export
470 less than 0.153 Tg C yr⁻¹ as DOC (reported as TOC, Butman et al., 2016). This suggests that the
471 hypermaritime coast of British Columbia plays an important role in the export of DOC from
472 coastal temperate rainforest ecosystems of western North America, in a region that is already
473 expected to contribute high quantities of DOC to the coastal ocean.

474 **4.2 DOM composition**

475 The composition of stream water DOM exported from Calvert and Hecate Island
476 watersheds is mainly terrestrial, indicating the production and overall supply of terrestrial
477 material is sufficient to exceed microbial demand, and thus a relatively abundant supply of
478 terrestrial DOM is available for export. Values for $\delta^{13}\text{C}$ -DOC suggest terrestrial carbon sources
479 from C3 plants and soils were the dominant input to catchment stream water DOM (Finlay and
480 Kendall, 2007). Measures of S_R and SUVA_{254} were typical of environments that export large
481 quantities of high molecular weight, highly aromatic DOM such as some tropical rivers (e.g.,

482 Lambert et al., 2016; Mann et al., 2014), streams draining wetlands (e.g., Ågren et al., 2008,
483 Austnes et al., 2010), or streams draining small undisturbed catchments comprised of mixed
484 forest and wetlands (e.g. Wickland et al., 2007; Fellman et al., 2009a; Spencer et al., 2010,
485 Yamashita et al., 2011). This suggests the majority of the DOM pool is comprised of larger
486 molecules that have not been extensively chemically or biologically degraded through processes
487 such as microbial utilization or photodegradation, and therefore are potentially more biologically
488 available (Amon and Benner, 1996).

489 Biological utilization of DOM is influenced by its composition (e.g. Judd et al., 2006;
490 Fasching et al., 2014), therefore differences in DOM can alter the downstream fate and
491 ecological role of freshwater-exported DOM. For example, the majority of the fluorescent DOM
492 pool was comprised of C1, which is described as humic-like, less-processed terrestrial soil and
493 plant material (see Table 2). In addition, although the tryptophan-like component C6, represents
494 a minor proportion of total fluorescence, even a small proteinaceous fraction of the overall DOM
495 pool can play a major role in overall bioavailability and bacterial utilization of DOM (Berggren
496 et al., 2010; Guillet and Giorgio, 2011). These contributions of stream-exported DOM may
497 represent a relatively fresh, seasonally-consistent contribution of terrestrial subsidy from streams
498 to the coastal ecosystem, which in this region is relatively lower in carbon and nutrients
499 throughout much of the year (Whitney et al., 2005; Johannessen et al., 2008).

500 **4.3. DOC and DOM export: Sources and seasonal variability**

501 On Calvert and Hecate Islands, the relationship between DOC concentration and
502 discharge varied by watershed (see Supplemental Fig. S6.1), as might be expected given the
503 known influence of watershed characteristics (e.g., lake area, wetland area, soils, etc) on DOC
504 concentration and export. However, overall DOC concentrations increased in all watersheds with
505 both discharge and temperature indicating the overarching drivers of DOC export are the
506 hydrologic coupling of precipitation and runoff from the landscape with the seasonal production
507 and availability of DOC (Fasching et al., 2016).

508 Precipitation is a well-established driver of stream DOC export (Alvarez-Cobelas et al.,
509 2012), particularly in systems containing organic soils and wetlands (Olefeldt et al., 2013; Wallin
510 et al., 2015; Leach et al., 2016). Frequent, high intensity precipitation events and short residence
511 times are expected to result in pulsed exports of stream DOC that are rapidly shunted

512 downstream, thus reducing time for in-stream processing (Raymond et al., 2016). Flashy stream
513 hydrographs indicate that hydrologic response times for Calvert and Hecate Island watersheds
514 are rapid, presumably as a result of small catchment size, high drainage density, and relatively
515 shallow soils with high hydraulic conductivity (Gibson et al., 2000; Fitzgerald et al., 2003).
516 Rapid runoff is presumably accompanied by rapid increases in water tables and lateral movement
517 of water through shallow soil layers rich in organic matter (Fellman et al., 2009b; D'Amore et
518 al., 2015b). It appears that on Calvert and Hecate Islands, the combination of high rainfall, rapid
519 runoff, and abundant sources of DOC from organic-rich wetlands and forests, result in high DOC
520 fluxes.

521 The relationship between DOC, stream temperature, and discharge indicates that seasonal
522 dynamics play an important role in the variability of DOC exported from these systems. For
523 example, DOC concentrations decrease in all watersheds during the wet period of the year, these
524 decreases are associated with clear changes in DOM composition, such as increasing $\delta^{13}\text{C-DOC}$,
525 SUVA_{254} , and decreasing S_R . This is in contrast with patterns observed during the dry period,
526 when DOC concentrations gradually increase, while $\delta^{13}\text{C-DOC}$, SUVA_{254} decrease. Fluctuations
527 in DOC and DOM composition occur throughout the wet and the dry season, suggesting that
528 temperature and runoff – and perhaps other seasonal drivers - are important year-round controls
529 on DOC concentration as well as certain measures of DOM composition, such as $\delta^{13}\text{C-DOC}$ and
530 S_R .

531 The process of “DOC flushing” has been shown to increase stream water DOC during
532 higher flows in coastal and temperate watersheds (e.g., Sanderman et al., 2009; Deirmendjian et
533 al., 2017). Flushing can occur through various mechanisms. For example, Boyer et al. (1996)
534 observed that during drier periods, DOC pools can increase in soils and are then flushed to
535 streams when water tables rise. Rising water tables can establish strong hydraulic gradients that
536 initiate and sustain prolonged increases in metrics like SUVA_{254} , until the progressive drawdown
537 of upland water tables constrain flow paths (Lambert et al., 2013). DOC concentrations can vary
538 during flushing in response to changing flow paths, which can shift sources of DOC within the
539 soil profile from older material in deeper soil horizons to more recently produced material in
540 shallow horizons (Sanderman et al., 2009), or from changes in the production mechanism of
541 DOC (Lambert et al., 2013). For example, Sanderman et al. (2009), observed distinct

542 relationships between discharge and both $\delta^{13}\text{C}$ -DOC and SUVA_{254} , and postulated that during
543 their rainy season, hillslope flushing shifts DOM sources to more aged soil organic material. In
544 addition, instream production can also provide a source of DOC, and therefore affect seasonal
545 variation in DOC concentration and composition (Lambert et al., 2013). The extent of these
546 effects can shift seasonally; relationships between flow paths and DOC export in rain-dominated
547 catchments can vary within and between hydrologic periods depending on factors such as the
548 degree of soil saturation, duration of previous drying and rewetting cycles, soil chemistry, and
549 DOM source-pool availability (Lambert et al., 2013).

550 Our observations of changes in DOC and DOM related to discharge and stream
551 temperature suggest that a variety of mechanisms may be important for controlling dynamics of
552 seasonal export in Pacific hypermaritime watersheds. We observed elevated DOC concentrations
553 during precipitation events following extended dry periods, suggesting DOC may accumulate
554 during dry periods and be flushed to streams during runoff events. Increased discharge was
555 significantly related to $\delta^{13}\text{C}$ -DOC and S_R , with higher discharge resulting in more terrestrial-like
556 DOM. One possible explanation is that hydrologic connectivity increases during higher
557 discharge as soil conditions become more saturated, therefore promoting the mobilization of
558 DOM from across a wider range of the soil profile (McKnight et al., 2001; Kalbitz et al., 2002).
559 In addition, the mechanisms of DOC production and sources of DOC appear to shift seasonally.
560 Relationships between increased temperature and lower values of $\delta^{13}\text{C}$ -DOC, and higher values
561 of Freshness Index, C1 and C4, suggest that warmer conditions result in a fresh supply of DOM
562 exported from terrestrial sources (Fellman et al., 2009a; Fasching et al., 2016). This may
563 represent a shift in the source of DOM and/or increased contributions from less aromatic, lower
564 molecular weight material, such as DOM derived from increased terrestrial primary production
565 (Berggren et al., 2010). Further, fine-scaled investigation into the mechanistic underpinnings of
566 the relationship between discharge, stream temperature, and DOM, represents a clear priority for
567 future research in this region.

568 **4.4 Relationships between watershed attributes and exported DOM**

569 Previous studies have implicated wetlands as a major driver of DOM composition (e.g.,
570 Xenopoulos et al., 2003; Ågren et al., 2008; Creed et al., 2008), however the analysis of
571 relationships between Calvert and Hecate Island landscape attributes and variation in DOM

572 composition suggests that controls on DOM composition are more nuanced than being solely
573 driven by the extent of wetlands. Ågren et al. (2008) found that when wetland area comprised
574 >10% of total catchment area, wetland DOM was the most significant driver of stream DOM
575 composition during periods of high hydrologic connectivity. Although wetlands comprise an
576 average of 37% of our study area, they do not appear to be the single leading driver of variability
577 in DOC concentration and DOM composition. Other factors, such as watershed slope, the depth
578 of organic and mineral soil materials, and the presence of lakes also appear to be influence DOC
579 concentration and DOM composition. The presence of cyptic wetlands (Creed et al., 2003) and
580 limitations of the wetland mapping method could also weaken the link between wetland extent,
581 DOC, and DOM.

582 In these watersheds, soils with pronounced accumulations of organic matter are not
583 restricted to wetland ecosystems. Peat accumulation in wetland ecosystems results in the
584 formation of organic soils (Hemists), where mobile fractions of DOM accumulate under
585 saturated soil conditions and limited drainage, resulting in the enrichment of poorly
586 biodegradable, more stable humic acids (Stevenson, 1994; Marschner and Kalbitz, 2003).
587 Although Hemist soils comprise 27.8% of our study area, Follic Histosols, which form under
588 more freely drained conditions, such as steeper slopes, occur over an additional 25.7% of the
589 area (Supplemental S1.2). In freely drained organic soils, high rates of respiration can result in
590 further enrichment of aromatic and more complex molecules, and this material may be rapidly
591 mobilized and exported to streams (Glatzel et al., 2003). This suggests the importance of widely
592 distributed, alternative soil DOM source-pools, such as Follic Histosols and associated Podzols
593 with thick forest floors on hillslopes, available to contribute high amounts of terrestrial carbon
594 for export.

595 Although lakes make up a relatively small proportion of the total landscape area, their
596 influence on DOM export appears to be important. The proportion of lake area can be a good
597 predictor of organic carbon loss from a catchment since lakes often increase hydrologic
598 residence times and thus increase opportunities for biogeochemical processing (Algesten et al.,
599 2004; Tranvik et al., 2009). In our study, watersheds with a larger percentage of lake area
600 exhibited slower response following rain events (Supplemental Fig. S2.2), lower DOC yields,
601 and lake area was correlated with parameters that represent greater autochthonous DOM

602 production or microbial processing such as higher Freshness Index, S_R , Fluorescence Index, and
603 higher proportions of component C6. In contrast, watersheds with a high percentage of wetlands
604 contributed DOM that was more allocthonous in composition. Lakes are known to be important
605 landscape predictors of DOC, as increased residence time enables removal via respiration, thus
606 reducing downstream exports from lake outlets (Larson et al., 2007). The proximity of wetlands
607 and lakes to the watershed outlet can also play an important role in the composition of DOM
608 exports (Martin et al., 2006).

609 **5 Conclusions**

610 Previous work has demonstrated freshwater discharge is substantial along the coastal
611 margin of the North Pacific temperate rainforest, and plays an important role in processes such as
612 ocean circulation (Royer, 1982; Eaton and Moore, 2010). Our finding that small catchments in
613 this region contribute high yields of terrestrial DOC to coastal waters suggests that freshwater
614 inputs may also influence ocean biogeochemistry and food web processes through terrestrial
615 organic matter subsidies. Our findings also suggest that this region may be currently
616 underrepresented in terms of its role in global carbon cycling. Currently, there is no region-wide
617 carbon flux model for the Pacific coastal temperate rainforest or the greater Gulf of Alaska,
618 which would quantify the importance of this region within the global carbon budget. Our
619 estimates point to the importance of the hypermaritime outer-coast zone of the CTR, where
620 subdued terrain, high rainfall, ocean moderated temperatures and poor bedrock have generated a
621 distinctive ‘bog-forest’ landscape mosaic within the greater temperate rainforest (Banner et al.
622 2005). However, even within our geographically limited study area, we observed a range of
623 DOC yields across watersheds. To quantify regional scale fluxes of rainforest carbon to the
624 coastal ocean, further research will be needed to estimate DOC yields across complex spatial
625 gradients of topography, climate, hydrology, soils and vegetation. Long term changes in DOC
626 flux have been observed in many places (e.g., Worrall et al., 2004; Borken et al., 2011; Lepistö et
627 al., 2014; Tank et al., 2016) and continued monitoring of this system will allow us to better
628 understand the underlying drivers of export and evaluate future patterns in DOC yields. Coupled
629 with current studies investigating the fate of terrestrial material in ocean food webs, this work
630 will improve our understanding of coastal carbon patterns, and increase capacity for predictions
631 regarding the ecological impacts of climate change.

632 **Author Contributions**

633 The authors declare that they have no conflict of interest.

634 A.A. Oliver prepared the manuscript with contributions from all authors, designed analysis
635 protocols, analyzed samples, performed the modeling and analysis for dissolved organic carbon
636 fluxes, parallel factor analysis of dissolved organic matter composition, and all remaining
637 statistical analyses. S.E. Tank assisted with designing the study and overseeing laboratory
638 analyses, crafting the scope of the paper, and determining the analytical approach.

639 I. Giesbrecht led the initial DOC sampling design, helped coordinate the research team, oversaw
640 routine sampling and data management, and led the watershed characterization.

641 M.C. Korver developed the rating curves, and conducted the statistical analysis of discharge
642 measurement uncertainties and rating curve uncertainties. W.C. Floyd lead the hydrology
643 component of this project, selected site locations, installed and designed the hydrometric
644 stations, and developed the rating curves and final discharge calculations. C. Bulmer and P.
645 Sanborn collected and analyzed soil field data and prepared the digital soils map of the
646 watersheds. K.P. Lertzman conceived of and co-led the overall study of which this paper is a
647 component, helped assemble and guide the team of researchers who carried out this work,
648 provided input to each stage of the study.

649

650 **Acknowledgements**

651 This work was funded by the Tula Foundation and the Hakai Institute. The authors would like to
652 thank many individuals for their support, including Skye McEwan, Bryn Fedje, Lawren McNab,
653 Nelson Roberts, Adam Turner, Emma Myers, David Norwell, and Chris Coxson for sample
654 collection and data management, Clive Dawson and North Road Analytical for sample
655 processing and data management, Keith Holmes for creating our maps, Matt Foster for database
656 development and support, Shawn Hateley for sensor network maintenance, Jason Jackson, Colby
657 Owen, James McPhail, and the entire staff at Hakai Energy Solutions for installing and
658 maintaining the sensors and telemetry network, and Stewart Butler and Will McInnes for field
659 support. Thanks to Santiago Gonzalez Arriola for generating the watershed summaries and
660 associated data products, and Ray Brunsting for overseeing the design and implementation of the
661 sensor network and the data management system at Hakai. Additional thanks to Lori Johnson

662 and Amelia Galuska for soil mapping field assistance, and Francois Guillet for PARAFAC
663 consultation. Thanks to Dave D'Amore for inspiring the Hakai project to investigate aquatic
664 fluxes at the coastal margin and for technical guidance. Lastly, thanks to Eric Peterson and
665 Christina Munck who provided significant guidance throughout the process of designing and
666 implementing this study.

667

668 **References**

669 Ågren, A., Buffam, I., Jansson, M. and Laudon, H.: Importance of seasonality and small streams
670 for the landscape regulation of dissolved organic carbon export, *J. Geophys. Res. Biogeosci.*,
671 112(G3), doi:10.1029/2006JG000381, 2007.

672

673 Ågren, A., Buffam, I., Berggren, M., Bishop, K., Jansson, M. and Laudon, H.: Dissolved organic
674 carbon characteristics in boreal streams in a forest-wetland gradient during the transition
675 between winter and summer, *J. Geophys. Res. Biogeosci.*, 113(G3), doi:10.1029/2007JG000674,
676 2008.

677

678 Akaike, H.: Likelihood of a model and information criteria, *J. Econometrics*, 16(1), 3-14,
679 doi:10.1016/0304-4076(81)90071-3, 1981.

680

681 Aitkenhead, J.A., and McDowell, W.H.: Soil C:N ratio as a predictor of annual riverine DOC
682 flux at local and global scales, *Global Biogeochem. Cycles*, 14(1), 127–138,
683 doi:10.1029/1999GB900083, 2000.

684

685 Alaback, P.B.: Biodiversity patterns in relation to climate: The coastal temperate rainforests of
686 North America, *Ecol. Stud.*, 116, 105–133, doi:10.1007/978-1-4612-3970-3_7, 1996.

687

688 Algesten, G., Sobek, S., Bergström, A., Ågren, A., Tranvik, L. and Jansson, M.: Role of lakes for
689 organic carbon cycling in the boreal zone, *Global Change Biol.*, 10(1), 141–147,
690 doi:10.1111/j.1365-2486.2003.00721.x, 2004.

691

692 Alvarez-Cobelas, M., Angeler, D., Sánchez-Carrillo, S. and Almendros, G.: A worldwide view
693 of organic carbon export from catchments, *Biogeochemistry*, 107(1-3), 275–293,
694 doi:10.1007/s10533-010-9553-z, 2012.

695

696 Amon, R.M.W., and Benner, R.: Bacterial utilization of different size classes of dissolved
697 organic matter, *Limnol. Oceanogr.*, 41, 41-51, 1996.

698

699 Aufdenkampe, A., Mayorga, E., Raymond, P., Melack, J., Doney, S., Alin, S., Aalto, R., and
700 Yoo, K.: Riverine coupling of biogeochemical cycles between land, oceans, and atmosphere,
701 *Front. Ecol. Environ.*, 9(1), 53–60, doi:10.1890/100014, 2011.

702

703 Austnes, K., Evans, C.D., Eliot-Laize, C., Naden, P.S., and Old, G.H.: Effects of storm events on
704 mobilisation and in-stream processing of dissolved organic matter (DOM) in a Welsh peatland
705 catchment, *Biogeochem.*, 99, 157-173, doi:10.1007/s10533-009-9399-4, 2010.
706

707 Banner, A., LePage, P., Moran, J., and de Groot, A. (Eds.): The HyP3 Project: pattern,
708 process, and productivity in hypermaritime forests of coastal British Columbia -
709 a synthesis of 7-year results, Special Report 10, Res. Br., British Columbia Ministry Forests,
710 Victoria, British Columbia, 142 pp., available at:
711 <http://www.for.gov.bc.ca/hfd/pubs/Docs/Srs/Srs10.htm>, 2005.
712

713 Battin, T.J., Kaplan, L.A., Findlay, S., Hopkinson, C.S., Marti, E., Packman, A.I., Newbold, D.,
714 and Sabater, F.: Biophysical controls on organic carbon fluxes in fluvial networks, *Nature*
715 *Geosci.*, 1, 95–100, 2008.
716

717 Bauer, J.E., Cai, W.J., Raymond, P.A., T.S., Bianchi, Hopkinson, C.S., and Regnier, P.A.G.: The
718 changing carbon cycle of the coastal ocean, *Nature*, 504(7478), 61-70, doi:10.1038/nature12857,
719 2013.
720

721 Berggren, M., Laudon, H., Haei, M., Ström, L., and Jansson, M.: Efficient aquatic bacterial
722 metabolism of dissolved low-molecular-weight compounds from terrestrial sources, *ISME J.*,
723 doi:10.1038/ismej.2009.120, 2010.
724

725 Boehme, J. and Coble, P.: Characterization of Colored Dissolved Organic Matter Using High-
726 Energy Laser Fragmentation, *Environ. Sci. Technology*, 34(15), 3283–3290,
727 doi:10.1021/es9911263, 2000.
728

729 Borcard, D., Gillet, F., and Legendre, P.: Numerical ecology with R, Springer, New York,
730 United States, doi:10.1007/978-1-4419-7976-6, 2011.
731

732 Borken, W., Ahrens, B., Schultz, C. and Zimmermann, L.: Site-to-site variability and temporal
733 trends of DOC concentrations and fluxes in temperate forest soils, *Global Change Biol.*, 17:
734 2428–2443, doi:10.1111/j.1365-2486.2011.02390.x, 2011.
735

736 Borges, A.V., Darchambeau, F., Teodoru, C.R., Marwick, T.R., Tamooh, F., Geeraert, N.,
737 Omengo, F.O., Guérin, F., Lambert, T., Morana, C., Okuku, E., and Bouillon, S.: Globally
738 significant greenhouse-gas emissions from African inland waters, *Nature Geosci.*, 8, 637–642,
739 doi:10.1038/ngeo2486, 2015.
740

741 Boyer, E.W., Hornberger, G.M., Bencala, K.E., and McKnight, D.: Overview of a simple model
742 describing variation of dissolved organic carbon in an upland catchment, *Ecol. Modell.*, 86, 183-
743 188, 1996.
744

745 Burnham K.P., and Anderson, D.R.: Model selection and multimodel inference, 2nd edn.
746 Springer, New York, 2002.
747

748 Carmack, E., Winsor, P., and William, W.: The contiguous panarctic Riverine Coastal Domain:
749 A unifying concept, *Prog. Oceanogr.*, 139, 13-23, doi:10.1016/j.pocean.2015.07.014, 2015.
750

751 Castillo, M.M., Allan, J.D., Sinsabaugh, R.L., and Kling, G.W.: Seasonal and interannual
752 variation of bacterial production in lowland rivers of the Orinoco basin, *Freshwater Biol.*, 49(11),
753 1400-1414, doi:10.1111/j.1365-2427.2004.01277.x, 2004.
754

755 Clark, J.M., Lane, S.N., Chapman, P.J., and Adamson, J.K.: Export of dissolved organic carbon
756 from an upland peatland during storm events: Implications for flux estimates, *J. Hydrol.*, 347(3-
757 4), 438-447, doi: 10.1016/j.jhydrol.2007.09.030, 2007.
758

759 Coble, P., Castillo, C. and Avril, B.: Distribution and optical properties of CDOM in the Arabian
760 Sea during the 1995 Southwest Monsoon, *Deep Sea Res. Part II, Oceanogr.*, 45(10-11), 2195–
761 2223, doi:10.1016/S0967-0645(98)00068-X, 1998.
762

763 Cole, J., Prairie, Y., Caraco, N., McDowell, W., Tranvik, L., Striegl, R., Duarte, C., Kortelainen,
764 P., Downing, J., Middelburg, J. and Melack, J.: Plumbing the Global Carbon Cycle: Integrating
765 Inland Waters into the Terrestrial Carbon Budget, *Ecosystems*, 10(1), 172–185,
766 doi:10.1007/s10021-006-9013-8, 2007.
767

768 Cory, R.M., and McKnight, D.M.: Fluorescence spectroscopy reveals ubiquitous presence of
769 oxidized and reduced quinines in dissolved organic matter, *Environ. Sci. Technol.*, 39, 8142 -
770 8149, doi:10.1021/es0506962, 2005.
771

772 Creed, I.F., Beall, F.D., Clair, T.A., Dillon, P.J., and Hesslein, R.H.: Predicting export of
773 dissolved organic carbon from forested catchments in glaciated landscapes with shallow soils,
774 *Glob. Biogeochem. Cycles*, 22, GB4024, doi:10.1029/2008GB003294, 2008.
775

776 Creed, I.F., Sanford, S.E., Beall, F.D., Molot, L.A., and Dillon, P.J.: Cryptic wetlands:
777 integrating hidden wetlands in regression models of the export of dissolved organic carbon from
778 forested landscapes, *Hydrol. Process.*, 17, 3629-3648, 2003.
779

780 D'Amore, D.V., Edwards, R.T., and Biles, F.E.: Biophysical controls on dissolved organic
781 carbon concentrations of Alaskan coastal temperate rainforest streams, *Aquat. Sci.*,
782 doi:10.1007/s00027-015-0441-4, 2015a.
783

784 D'Amore, D.V., Edwards, R.T., Herendeen, P.A., Hood, E., and Fellman, J.B.: Dissolved
785 organic carbon fluxes from hydrogeologic units in Alaskan coastal temperate rainforest
786 watersheds, *Soil Sci. Soc. Am. J.*, 79:378-388, doi:10.2136/sssaj2014.09.0380, 2015b.
787

788 D'Amore, D.V., Biles, F.E., Nay, M., Rupp, T.S.: Watershed carbon budgets in the southeastern
789 Alaskan coastal forest region, in: *Baseline and projected future carbon storage and greenhouse-
790 gas fluxes in ecosystems of Alaska*, U.S. Geological Survey Professional Paper, 1826, 196 p.,
791 2016.
792

793 Dai, M., Yin, Z., Meng, F., Liu, Q. and Cai, W.J.: Spatial distribution of riverine DOC inputs to
794 the ocean: an updated global synthesis, *Curr. Opin. Sust.*, 4(2), 170–178,
795 doi:10.1016/j.cosust.2012.03.003, 2012.

796

797 Deirmendjian, L., Loustau, D., Augusto, L., Lafont, S., Chipeaux, C., Poirier, D., and Abril, G.:
798 Hydrological and ecological controls on dissolved carbon concentrations in groundwater and
799 carbon export to surface waters in a temperate pine forest watershed, *Biogeosciences*
800 *Discuss.*, doi:10.5194/bg-2017-90, in review, 2017.

801

802 DellaSala, D.A.: *Temperate and Boreal Rainforests of the World*, Island Press, Washington,
803 D.C., 2011.

804

805 Emili, L. and Price, J.: Biogeochemical processes in the soil-groundwater system of a forest-
806 peatland complex, north coast British Columbia, Canada, *Northwest Sci.*, 88, 326–348,
807 doi:10.3955/046.087.0406, 2013.

808

809 Fasching, C., Behounek, B., Singer, G. and Battin, T.: Microbial degradation of terrigenous
810 dissolved organic matter and potential consequences for carbon cycling in brown-water streams,
811 *Sci. Rep.*, 4, 4981, doi:10.1038/srep04981, 2014.

812

813 Fasching, C., Ulseth, A., Schelker, J., Steniczka, G. and Battin, T.: Hydrology controls dissolved
814 organic matter export and composition in an Alpine stream and its hyporheic zone, *Limnol.*
815 *Oceanogr.*, 61(2), 558–571, doi:10.1002/lno.10232, 2016.

816

817 Fellman, J., Hood, E., D’Amore, D., Edwards, R. and White, D.: Seasonal changes in the
818 chemical quality and biodegradability of dissolved organic matter exported from soils to streams
819 in coastal temperate rainforest watersheds, *Biogeochemistry*, 95, 277–293, doi:10.1007/s10533-
820 009-9336-6, 2009a.

821

822 Fellman, J., Hood, E., Edwards, R. and D’Amore, D.: Changes in the concentration,
823 biodegradability, and fluorescent properties of dissolved organic matter during stormflows in
824 coastal temperate watersheds, *J. Geophys. Res. Biogeosci.*, 114, doi:10.1029/2008JG000790,
825 2009b.

826

827 Fellman, J., Hood, E. and Spencer, R.: Fluorescence spectroscopy opens new windows into
828 dissolved organic matter dynamics in freshwater ecosystems: A review, *Limnol. Oceanogr.*, 55,
829 24522462, doi:10.4319/lno.2010.55.6.2452, 2010.

830

831 Fellman, J., Nagorski, S., Pyare, S., Vermilyea, A.W., Scott, D., and Hood, E.: Stream
832 temperature response to variable glacier cover in coastal watersheds of Southeast Alaska,
833 *Hydrol. Process.*, 28, 2062-2073, doi:10.1002/hyp.9742, 2014

834

835 Finlay, J.C., and Kendall, C.: Stable isotope tracing of temporal and spatial variability in organic
836 matter sources and variability in organic matter sources to freshwater ecosystems, in *Stable*
837 *Isotopes in Ecology and Environmental Science*, 2, Michener, R., and Lajtha, K. (Eds),
838 Blackwell Publishing Ltd, Oxford, UK, 283-324, 2007.

839
840 Fitzgerald, D., Price, J., and Gibson, J.: Hillslope-swamp interactions and flow pathways in a
841 hypermaritime rainforest, British Columbia, *Hydrol. Process.*, 17, 3005-3022,
842 doi:10.1002/hyp.1279, 2003.
843
844 Gibson, J.J., Price, J.S., Aravena, R., Fitzgerald, D.F., and Maloney, D.: Runoff generation in a
845 hypermaritime bog-forest upland, *Hydrol. Process*, 14, 2711-2730, doi: 10.1002/1099-
846 1085(20001030)14:15<2711::AID-HYP88>3.0.CO;2-2, 2000.
847
848 Glatzel, S., Kalbitz, K., Dalva, M., and Moore, T.: Dissolved organic matter properties and their
849 relationship to carbon dioxide efflux from restored peat bogs, *Geoderma*, 113, 397-411, 2003.
850
851 Gonzalez Arriola S., Frazer, G.W., Giesbrecht, I.: LiDAR-derived watersheds and their metrics
852 for Calvert Island, Hakai Institute, doi:dx.doi.org/10.21966/1.15311, 2015.
853
854 Gorham, E., Lehman, C., Dyke, A., Clymo, D., and Janssens, J.: Long-term carbon sequestration
855 in North American peatlands, *Quat. Sci. Review*, 58, 77-82, 2012.
856
857 Graeber, D., Gelbrecht, J., Pusch, M., Anlanger, C. and von Schiller, D.: Agriculture has
858 changed the amount and composition of dissolved organic matter in Central European headwater
859 streams, *Sci. Total Environ.*, 438, 435–446, doi:10.1016/j.scitotenv.2012.08.087, 2012.
860
861 Green, R.N.: Reconnaissance level terrestrial ecosystem mapping of priority landscape units of
862 the coast EBM planning area: Phase 3, Prepared for British Columbia Ministry Forests, Lands
863 and Natural Resource Ops., Blackwell and Associates, Vancouver, Canada, 2014.
864
865 Guillemette, F. and Giorgio, P.: Reconstructing the various facets of dissolved organic carbon
866 bioavailability in freshwater ecosystems, *Limnol. Oceanogr.*, 56, 734–748,
867 doi:10.4319/lo.2011.56.2.0734, 2011.
868
869 Hansen, A.M., Kraus, T.E.C., Pellerin, B.A., Fleck, J.A., Downing, B.D., and Bergamaschi,
870 B.A.: Optical properties of dissolved organic matter (DOM): Effects of biological and photolytic
871 degradation, *Limnol. Oceanogr.*, 61, 1015-1032, doi:10.1002/lno.10270, 2016.
872
873 Harrell, F.E., Dupont, C., and many others.: Hmisc: Harrell Miscellaneous. R package version
874 4.0-2. <https://CRAN.R-project.org/package=Hmisc>, 2016.
875
876 Harrison, J., Caraco, N. and Seitzinger, S.: Global patterns and sources of dissolved organic
877 matter export to the coastal zone: Results from a spatially explicit, global model, *Global*
878 *Biogeochem. Cycles*, 19, doi:10.1029/2005gb002480, 2005.
879
880 Helms, J., Stubbins, A., Ritchie, J., Minor, E., Kieber, D. and Mopper, K.: Absorption spectral
881 slopes and slope ratios as indicators of molecular weight, source, and photobleaching of
882 chromophoric dissolved organic matter, *Limnol. Oceanogr.*, 53, 955–969,
883 doi:10.4319/lo.2008.53.3.0955, 2008.
884

885 Helton, A., Wright, M., Bernhardt, E., Poole, G., Cory, R. and Stanford, J.: Dissolved organic
886 carbon lability increases with water residence time in the alluvial aquifer of a river floodplain
887 ecosystem, *J. Geophys. Res. Biogeosciences*, 120, 693–706, doi:10.1002/2014JG002832, 2015.
888

889 Hoffman, K.M., Gavin, D.G., Lertzman, K.P., Smith, D.J., and Starzomski, B.M.: 13,000 years
890 of fire history derived from soil charcoal in a British Columbia coastal temperate rain forest,
891 *Ecosphere*, 7, e01415, doi:10.1002/ecs2.1415, 2016.
892

893 Hope, D., Billett, M.F., and Cresser, M.S.: A review of the export of carbon in river water:
894 Fluxes and processes, *Environ. Pollut.*, 84(3), 301-324, doi:10.1016/0269-7491(94)90142-2,
895 1994.
896

897 Hopkinson, C.S., Buffam, I., Hobbie, J., Vallino, J. and Perdue, M.: Terrestrial inputs of organic
898 matter to coastal ecosystems: An intercomparison of chemical characteristics and bioavailability,
899 *Biogeochemistry*, 43, 211–234, 1998.
900

901 Hudson, N., Baker, A. and Reynolds, D.: Fluorescence analysis of dissolved organic matter in
902 natural, waste and polluted waters-a review, *River Res. Appl.*, 23, 631–649,
903 doi:10.1002/rra.1005, 2007.
904

905 Hurvich, C.M., and Tsai, C.: Regression and time series model selection in small samples,
906 *Biometrika*, 76(2), 297-307, doi:10.2307/2336663, 1989.
907

908 International Union of Soil Sciences (IUSS) Working Group: World Reference Base for Soil
909 Resources, International soil classification system for naming soils and creating legends for soil
910 maps, World Soil Resources Reports No. 106, Food and Agricultural Organization of the United
911 Nations, Rome, Italy, 2015.
912

913 ISO Standard 9196: Liquid flow measurement in open channels - Flow measurements under ice
914 conditions, International Organization for Standardization, available online at www.iso.org,
915 1992.
916

917 ISO Standard 748: Hydrometry - Measurement of liquid flow in open channels using current-
918 meters or floats, International Organization for Standardization, available online at www.iso.org,
919 2007.
920

921 Johannessen, S.C., Potentier, G., Wright, C.A., Masson, D., and Macdonald, R.W.: Water
922 column organic carbon in a Pacific marginal sea (Strait of Georgia, Canada), *Mar. Environ. Res.*,
923 66, S49-S61, doi:10.1016/j.marenvres.2008.07.008, 2008.
924

925 Johnson, P.C.D.: Extension of Nakagawa & Schielzeth's R^2_{GLMM} to random slopes models.
926 *Methods Ecol. Evol.*, DOI: 10.1111/2041-210X.12225, 2014.
927

928 Johnson, M., Couto, E., Abdo, M. and Lehmann, J.: Fluorescence index as an indicator of
929 dissolved organic carbon quality in hydrologic flowpaths of forested tropical watersheds,
930 *Biogeochemistry*, 105, 149–157, doi:10.1007/s10533-011-9595-x, 2011.

931
932 Judd, K., Crump, B. and Kling, G.: Variation in dissolved organic matter controls bacterial
933 production and community composition, *Ecology*, 87, 2068–2079, doi:10.1890/0012-
934 9658(2006)87[2068:VIDOMC]2.0.CO;2, 2006.
935
936 Kalbitz, K., Schmerwitz, J., Schwesig, D. and Matzner, E.: Biodegradation of soil-derived
937 dissolved organic matter as related to its properties, *Geoderma*, 113, 273–291,
938 doi:10.1016/S0016-7061(02)00365-8, 2003.
939
940 Kling, G., Kipphut, G., Miller, M. and O'Brien, W.: Integration of lakes and streams in a
941 landscape perspective: the importance of material processing on spatial patterns and temporal
942 coherence, *Freshwater Biol.*, 43, 477–497, doi:10.1046/j.1365-2427.2000.00515.x, 2000.
943
944 Koehler, A.-K., Murphy, K., Kiely, G. and Sottocornola, M.: Seasonal variation of DOC
945 concentration and annual loss of DOC from an Atlantic blanket bog in South Western Ireland,
946 *Biogeochemistry*, 95, 231–242, doi:10.1007/s10533-009-9333-9, 2009.
947
948 Lakowicz, J.R.: *Principles of Fluorescence Spectroscopy*, 2, Kluwer Academic, New York,
949 1999.
950
951 Larson, J.H., Frost, P.C., Zheng, Z., Johnston, C.A., Bridgham, S.D., Lodge, D.M., and
952 Lamberti, G.A.: Effects of upstream lakes on dissolved organic matter in streams, *Limnol.*
953 *Oceanogr.*, 52(1), 60-69, doi:10.4319/lo.2007.52.1.0060, 2007.
954
955 Leighty, W.W., Hamburg, S.P., and Caouette, J.: Effects of management on carbon sequestration
956 in forest biomass in Southeast Alaska, *Ecosystems*, 9, 1051, doi:10.1007/s10021-005-0028-3,
957 2006.
958
959 Lalonde, K., Middlestead, P., Gélinas, Y.: Automation of ¹³C/¹²C ratio measurement for
960 freshwater and seawater DOC using high temperature combustion, *Limnol. Oceanogr. Methods*,
961 12, 816-829, doi:10.4319/lom.2014.12.816, 2014.
962
963 Lambert, T., Bouillon, S., Darchambeau, F., Massicotte, P., and Borges, A.V.: Shift in the
964 chemical composition of dissolved organic matter in the Congo River network, *Biogeosci.*, 13,
965 5405-5420, doi:10.5194/bg-13-5405-2016, 2016.
966
967 Leach, J., Larsson, A., Wallin, M., Nilsson, M. and Laudon, H.: Twelve year interannual and
968 seasonal variability of stream carbon export from a boreal peatland catchment, *J. Geophys. Res.*
969 121, 1851–1866, doi:10.1002/2016JG003357, 2016.
970
971 Legendre, P., and Durand, S.: rdaTest, Canonical redundancy analysis, R package version 1.11,
972 available at <http://adn.biol.umontreal.ca/~numerica/ecology/Rcode/>, 2014.
973
974 Lepistö, A., Futter, M.N. and Kortelainen, P.: Almost 50 years of monitoring shows that climate,
975 not forestry, controls long-term organic carbon fluxes in a large boreal watershed, *Glob. Change*
976 *Biol.*, 20, 1225–1237, doi:10.1111/gcb.12491, 2014.

977
978 Liaw, A., and Wiener, M.: Classification and Regression by randomForest, R News, 2(3), 18-22,
979 2002.
980
981 Lochmuller, C.H., Saavedra, S.S.: Conformational changes in a soil fulvic acid measured by time
982 dependent fluorescence depolarization, Anal. Chem., 38, 1978-1981, 1986.
983
984 Lorenz, D., Runkel, R., and De Cicco, L.: rloadest, River Load Estimation, R package version
985 0.4.2, available at <https://github.com/USGS-R/rloadest>, 2015.
986
987 Ludwig, W., Probst, J. and Kempe, S.: Predicting the oceanic input of organic carbon by
988 continental erosion, Global Biogeochem. Cycles, 10, 23–41, doi:10.1029/95GB02925, 1996.
989
990 Mann, P.J., Spencer, R.G.M., Dinga, B.J., Poulsen, J.R., Hernes, P.J., Fiske, G., Salter, M.E.,
991 Wang, Z.A., Hoering, K.A., Six, J., and Holmes, R.M.: The biogeochemistry of carbon across a
992 gradient of streams and rivers within the Congo Basin, J. Geophys. Res. Biogeosci., 119, 687-
993 702, doi:10.1002/2013JG002442, 2014.
994
995 Marschner, B., and Kalbitz, K.: Controls on bioavailability and biodegradability of dissolved
996 organic matter in soils, Geoderma, 113, 211–235, 2003.
997
998 Martin, S.L., and Soranno, P.A.: Lake landscape position: Relationships to hydrologic
999 connectivity and landscape features, Limnol. Oceanogr., 51(2), 801-814,
1000 doi:10.4319/lo.2006.51.2.0801, 2006.
1001
1002 Masiello, C.A., and Druffel, E.R.M.: Carbon isotope geochemistry of the Santa Clara River,
1003 Global Biogeochem. Cycles, 15, 407-416, doi:10.1029/2000GB001290, 2001.
1004
1005 Mayorga, E., Seitzinger, S., Harrison, J., Dumont, E., Beusen, A., Bouwman, A.F., Fekete, B.,
1006 Kroeze, C. and Drecht, G.: Global Nutrient Export from WaterSheds 2 (NEWS 2): Model
1007 development and implementation, Environ. Model. Softw., 25, 837–853,
1008 doi:10.1016/j.envsoft.2010.01.007, 2010.
1009
1010 McClelland, J., Townsend-Small, A., Holmes, R., Pan, F., Stieglitz, M., Khosh, M. and Peterson,
1011 B.: River export of nutrients and organic matter from the North Slope of Alaska to the Beaufort
1012 Sea, Water Resour. Res., 50, 1823–1839, doi:10.1002/2013WR014722, 2014.
1013
1014 McKnight, D., Boyer, E., Westerhoff, P., Doran, P., Kulbe, T. and Andersen, D.:
1015 Spectrofluorometric characterization of dissolved organic matter for indication of precursor
1016 organic material and aromaticity, Limnol. Oceanogr., 46, 38–48, doi:10.4319/lo.2001.46.1.0038,
1017 2001.
1018
1019 McLaren, D., Fedje, D., Hay, M.B., Mackie, Q., Walker, I.J., Shugar, D.H., Eamer, J.B.R., Lian,
1020 O.B., and Neudorf, C.: A post-glacial sea level hinge on the central Pacific coast of Canada,
1021 Quat. Sci. Review., 97, 148-169, 2014.

1022
1023 Meybeck, M.: Carbon, nitrogen, and phosphorus transport by world rivers, *Am. J. Sci.*, 282, 401-
1024 450, Available from: <http://earth.geology.yale.edu/~ajs/1982/04.1982.01.Maybeck.pdf>, 1982.
1025
1026 Milliman, J.D., and Syvitski J.P.M.: Geomorphic tectonic control of sediment discharge to the
1027 ocean: The importance of small mountainous rivers, *J. Geol.*, 100, 525-544, 1992.
1028
1029 Moore, R.D.: Introduction to salt dilution gauging for streamflow measurement part III: Slug
1030 injection using salt in solution, *Streamline Watershed Management Bulletin*, 8(2), 1-6, 2005.
1031
1032 Morrison, J., Foreman, M.G.G., and Masson, D.: A method for estimating monthly freshwater
1033 discharge affecting British Columbia coastal waters, *Atmosphere-Ocean*, 50, 1-8,
1034 doi:10.1080/07055900.2011.637667, 2012.
1035
1036 Mulholland, P. and Watts, J.: Transport of organic carbon to the oceans by rivers of North
1037 America: a synthesis of existing data, *Tellus*, 34, 176–186, doi:10.1111/j.2153-
1038 3490.1982.tb01805.x, 1982.
1039
1040 Murphy, K., Stedmon, C., Graeber, D. and Bro, R.: Fluorescence spectroscopy and multi-way
1041 techniques. PARAFAC, *Anal. Methods*, 5, 6557–6566, doi:10.1039/C3AY41160E, 2013.
1042
1043 Murphy K., Stedmon, C., Wenig, P., Bro, R.: OpenFluor- A spectral database of auto-
1044 fluorescence by organic compounds in the environment, *Anal. Methods*, 6, 658-661,
1045 DOI:10.1039/C3AY41935E, 2014.
1046
1047 Naiman, R.J.: Characteristics of sediment and organic carbon export from pristine boreal forest
1048 watersheds, *Can. J. Fish. Aquat. Sci.*, 39(12), 1699-1718, doi:10.1139/f82-226, 1982.
1049
1050 Nakagawa, S., and Schielzeth, H.: A general and simple method for obtaining R^2 from
1051 generalized linear mixed-effects models, *Methods Ecol. Evol.*, 4(2): 133-
1052 142. DOI: 10.1111/j.2041-210x.2012.00261.x, 2013.
1053
1054 Olefeldt, D., Roulet, N., Giesler, R. and Persson, A.: Total waterborne carbon export and DOC
1055 composition from ten nested subarctic peatland catchments- importance of peatland cover,
1056 groundwater influence, and inter-annual variability of precipitation patterns, *Hydrol. Process.*,
1057 27, 2280-2294, doi:10.1002/hyp.9358, 2013.
1058
1059 Pinheiro, J., Bates, D., DebRoy, S., Sarkar, D., and R Core Team: nlme: Linear and Nonlinear
1060 Mixed Effects Models, R package version 3.1-128, 2016.
1061
1062 Pojar, J., Klinka, K., and Demarchi, D.A.: Chapter 6, Coastal Western Hemlock Zone, in:
1063 Special Report Series 6, Ecosystems of British Columbia, Meidiner, D., and Pojar, J. (Eds.),
1064 Ministry of Forests, British Columbia, Victoria, 330 p., 1991.
1065
1066 Poulin, B., Ryan, J. and Aiken, G.: Effects of iron on optical properties of dissolved organic
1067 matter, *Environ. Sci. Technol.*, 48, 10098–106, doi:10.1021/es502670r, 2014.

1068
1069 R Core Team, R: A language and environment for statistical computing, R Foundation for
1070 Statistical Computing, Vienna, Austria, <http://www.R-project.org/>, 2013.
1071
1072 Raymond, P., Saiers, J. and Sobczak, W.: Hydrological and biogeochemical controls on
1073 watershed dissolved organic matter transport: pulse-shunt concept, *Ecology*, 97, 5-16,
1074 doi:10.1890/14-1684.1, 2016.
1075
1076 Regnier, P., Friedlingstein, P., Ciais, P., Mackenzie, F., Gruber, N., Janssens, I., Laruelle, G.,
1077 Lauerwald, R., Luysaert, S., Andersson, A., Arndt, S., Arnosti, C., Borges, A., Dale, A.,
1078 Gallego-Sala, A., Godd ris, Y., Goossens, N., Hartmann, J., Heinze, C., Ilyina, T., Joos, F.,
1079 LaRowe, D., Leifeld, J., Meysman, F., Munhoven, G., Raymond, P., Spahni, R., Suntharalingam,
1080 P. and Thullner, M.: Anthropogenic perturbation of the carbon fluxes from land to ocean, *Nat.*
1081 *Geosci.*, 6, 597–607, doi:10.1038/ngeo1830, 2013.
1082
1083 Roddick, J.R.: Geology, Rivers Inlet-Queens Sound, British Columbia, Open File 3278,
1084 Geological Survey of Canada, Ottawa, Canada, 1996.
1085
1086 Royer, T.C., Coastal fresh water discharge in the northeast, Pacific, *J. Geophys. Res.*, 87, 2017-
1087 2021, 1982.
1088
1089 Runkel, R.L., Crawford, C.G., and Cohn, T.A.: Load Estimator (LOADEST): A FORTRAN
1090 program for estimating constituent loads in streams and rivers, U.S. Geological Survey
1091 Techniques and Methods Book 4, Chapter A5, 65 pp., 2004.
1092
1093 Sanderman, J., Lohse, K.A., Baldock, J.A., and Amundson, R.: Linking soils and streams:
1094 Sources and chemistry of dissolved organic matter in a small coastal watershed, *Water Resour.*
1095 *Res.*, 45, W03418, doi:10.1029/2008WR006977, 2009.
1096
1097 Spencer, R., Butler, K. and Aiken, G.: Dissolved organic carbon and chromophoric dissolved
1098 organic matter properties of rivers in the USA, *J. Geophys. Res. Biogeosciences*, 117(G03001),
1099 doi:10.1029/2011JG001928, 2012.
1100
1101 Spencer, R.G., Hernes, P.J, Ruf, R., Baker, A., Dyda, R.Y., Stubbins, A., and Six, J.: Temporal
1102 controls on dissolved organic matter and lignin biogeochemistry in a pristine tropical river,
1103 Democratic Republic of Congo, *J. Geophys. Res.*, 115, G03013, doi:10.1029/2009JG001180,
1104 2010.
1105
1106 Stackpoole, S.M., Butman, D.E., Clow, D.W., Verdin, K.L., Gaglioti, B., and Striegl, R.: Carbon
1107 burial, transport, and emission from inland aquatic ecosystems in Alaska, in: Baseline and
1108 projected future carbon storage and greenhouse-gas fluxes in ecosystems of Alaska, Zhiliang, Z.,
1109 and David, A. (Eds.), U.S. Geological Survey Professional Paper, 1826, 196 p., 2016.
1110
1111 Stackpoole, S.M., Butman, D.E., Clow, D.W., Verdin, K.L., Gaglioti, B.V., Genet, H., and
1112 Striegl, R.G.: Inland waters and their role in the carbon cycle of Alaska, *Ecol. Appl.*, Accepted
1113 Author Manuscript, doi: 10.1002/eap.1552, 2017.

1114
1115 Stedmon, C. and Bro, R.: Characterizing dissolved organic matter fluorescence with parallel
1116 factor analysis: a tutorial, *Limnol. Oceanogr. Methods*, 6, 572–579,
1117 doi:10.4319/lom.2008.6.572b, 2008.
1118
1119 Stedmon, C. and Markager, S.: Tracing the production and degradation of autochthonous
1120 fractions of dissolved organic matter by fluorescence analysis, *Limnol. Oceanogr.*, 50(5), 1415–
1121 1426, doi:10.4319/lo.2005.50.5.1415, 2005.
1122
1123 Stedmon, C., Markager, S., Bro, R., Stedmon, C., Markager, S. and Bro, R.: Tracing dissolved
1124 organic matter in aquatic environments using a new approach to fluorescence spectroscopy, *Mar.*
1125 *Chem.*, doi:10.1016/S0304-4203(03)00072-0, 2003.
1126
1127 Stevenson, F.J.: *Humus Chemistry: Genesis, Composition, Reactions*, 2, Jon Wiley and Sons
1128 Inc., New York, United States of America, 1994.
1129
1130 Symonds, M.R.E., and Moussalli, A.: A brief guide to model selection, multimodel inference,
1131 and model averaging in behavioural ecology using Akaike’s information criterion, *Behav. Ecol.*
1132 *Sociobiol.*, 65:13-21, DOI: 10.1007/s00265-010-1037-6, 2011.
1133
1134 Tallis, H.: Kelp and rivers subsidize rocky intertidal communities in the Pacific Northwest
1135 (USA), *Marine Ecology Progress Series*, 389, 8596, doi:10.3354/meps08138, 2009.
1136
1137 Tank, S., Raymond, P., Striegl, R., McClelland, J., Holmes, R., Fiske, G. and Peterson, B.: A
1138 land-to-ocean perspective on the magnitude, source and implication of DIC flux from major
1139 Arctic rivers to the Arctic Ocean, *Global Biogeochem. Cycles*, 26, GB4018,
1140 doi:10.1029/2011GB004192, 2012.
1141
1142 Tank, S., Striegl, R.G., McClelland, J.W., and Kokelij, S.V.: Multi-decadal increases in
1143 dissolved organic carbon and alkalinity flux from the Mackenzie drainage basin to the Arctic
1144 Ocean, *Environ. Res. Lett.*, 11(5), doi:10.1088/1748-9326/11/5/054015, 2016.
1145
1146 Thompson, S.D., Nelson, T.A., Giesbrecht, I., Frazer, G., and Saunders, S.C.: Data-driven
1147 regionalization of forested and non-forested ecosystems in coastal British Columbia with LiDAR
1148 and RapidEye imagery, *Appl. Geogr.*, 69, 35–50, doi: 10.1016/j.apgeog.2016.02.002,
1149 2016.
1150
1151 Trant, A.J., Nijland, W., Hoffman, K.M., Mathews, D.L., McLaren, D., Nelson, T.A.,
1152 Starzomski, B.M.: Intertidal resource use over millennia enhances forest productivity, *Nature*
1153 *Commun.*, 7, 12491, doi: 10.1038/ncomms12491, 2016.
1154
1155 van Hees, P., Jones, D., Finlay, R., Godbold, D. and Lundström, U.: The carbon we do not see-
1156 the impact of low molecular weight compounds on carbon dynamics and respiration in forest
1157 soils: a review, *Soil Biol. Biochem.*, 37, 1–13, doi:10.1016/j.soilbio.2004.06.010, 2005.
1158

1159 Wallin, M., Weyhenmeyer, G., Bastviken, D., Chmiel, H., Peter, S., Sobek, S. and Klemetsson,
1160 L.: Temporal control on concentration, character, and export of dissolved organic carbon in two
1161 hemiboreal headwater streams draining contrasting catchments, *J. Geophys. Res. Biogeosci.* 120,
1162 832–846, doi:10.1002/2014jg002814, 2015.

1163
1164 Wang, T., Hamann, A., Spittlehouse, D.L., and Murdock, T.Q.: ClimateWNA- High resolution
1165 spatial climate data for Western North America, *J. Appl. Meteorol. Climatol.*, 51, 16-29,
1166 doi:dx.doi.org/10.1175/JAMC-D-11-043.1, 2012.

1167
1168 Weishaar, J.L., Aiken, G.R., Bergamaschi, B.A., Fram, M.S., Fujii, R. and Mopper, K.:
1169 Evaluation of specific ultraviolet absorbance as an indicator of the chemical composition and
1170 reactivity of dissolved organic carbon, *Environ. Sci. Technol.*, 37, 4702–4708,
1171 doi:10.1021/es030360x, 2003.

1172
1173 Whitney, F.A., Crawford, W.R. and Harrison, P.J.: Physical processes that enhance nutrient
1174 transport and primary productivity in the coastal and open ocean of the subarctic NE
1175 Pacific, *Deep Sea Research Part II: Topical Studies in Oceanography*, 52, 681–706, 2005.

1176
1177 Wickland, K., Neff, J., and Aiken, G.: Dissolved Organic Carbon in Alaskan Boreal Forest:
1178 Sources, Chemical Characteristics, and Biodegradability, *Ecosystems*, 10, 1323-1340, 2007.

1179
1180 Wilson, H.F. and Xenopoulos, M.A.: Effects of agricultural land use on the composition of
1181 fluvial dissolved organic matter, *Nat. Geosci.*, 2, 37–41, doi:10.1038/ngeo391, 2009.

1182
1183 Wolf, E.C., Mitchell, A.P., and Schoonmaker, P.K.: *The Rain Forests of Home: An Atlas of*
1184 *People and Place*, Ecotrust, Pacific GIS, Inforain, and Conservation International, Portland,
1185 Oregon, 24 pp., available at: http://www.inforain.org/pdfs/ctrf_atlas_orig.pdf, 1995.

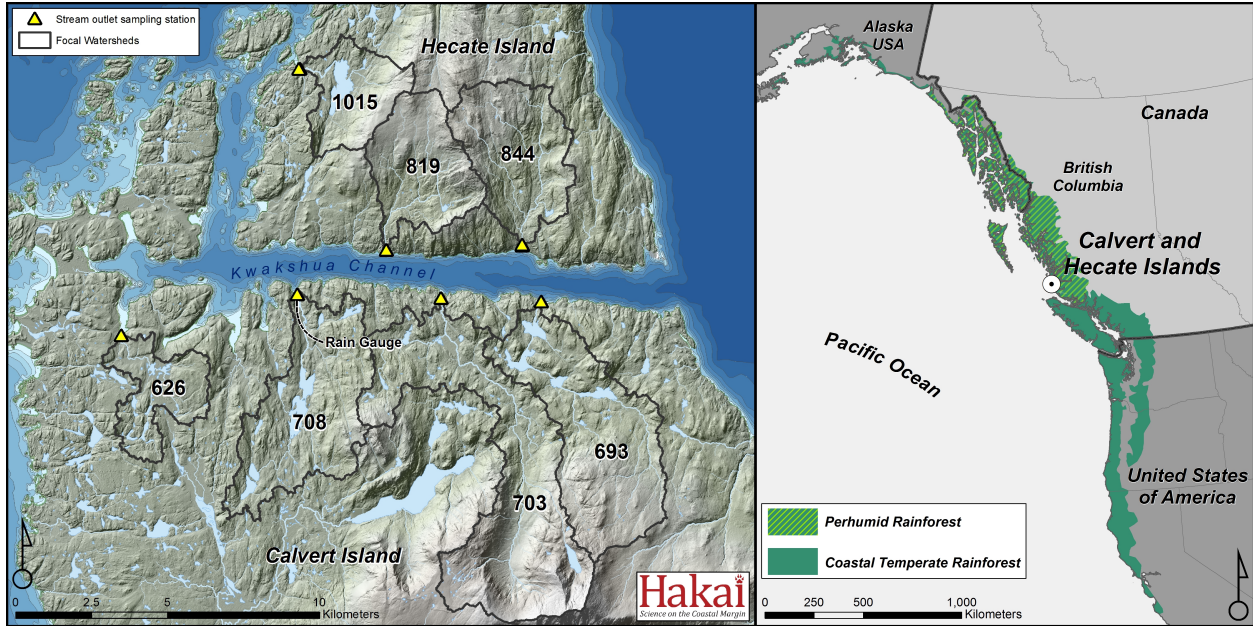
1186
1187 Worrall, F., Burt, T., and Adamson, J.: Can climate change explain increases in DOC flux from
1188 upland peat catchments?, *Sci. Total. Environ.*, 326, 95–112,
1189 doi:10.1016/j.scitotenv.2003.11.022, 2004.

1190
1191 Xenopoulos, M.A., Lodge, D.M., Frentress, J., Kreps, T.A., Bridgham, S.D., Grossman, E., and
1192 Jackson, C.J.: Regional comparisons of watershed determinants of dissolved organic carbon in
1193 temperate lakes from the Upper Great Lakes region and selected regions globally, *Limnol.*
1194 *Oceanogr.*, 48(6), 2321-2334, 2003.

1195
1196 Yamashita, Y. and Jaffé, R.: Characterizing the Interactions between Trace Metals and Dissolved
1197 Organic Matter Using Excitation–Emission Matrix and Parallel Factor Analysis, *Environ. Sci.*
1198 *Technol.*, 42, 7374–7379, doi:10.1021/es801357h, 2008.

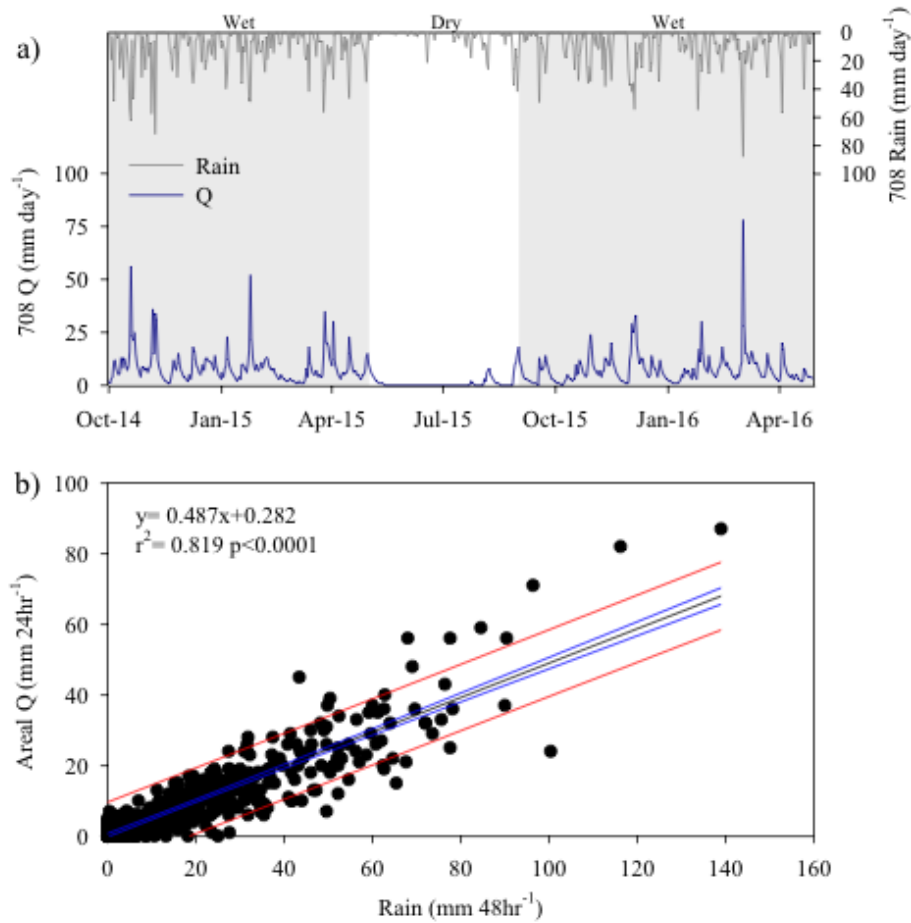
1199
1200 Yamashita, Y., Kloeppel, B., Knoepp, J., Zausen, G. and Jaffé, R.: Effects of Watershed History
1201 on Dissolved Organic Matter Characteristics in Headwater Streams, *Ecosystems*, 14, 1110–1122,
1202 doi:10.1007/s10021-011-9469-z, 2011.

1203 **Figure 1.** The location of Calvert Island, British Columbia, Canada, within the perhumid region
1204 of the coastal temperate rainforest (right) and the study area on Calvert and Hecate Islands,
1205 including the seven study watersheds, corresponding stream outlet sampling stations, and
1206 location of the rain gauge (left). Characteristics of individual watersheds are described in Table
1207 1.



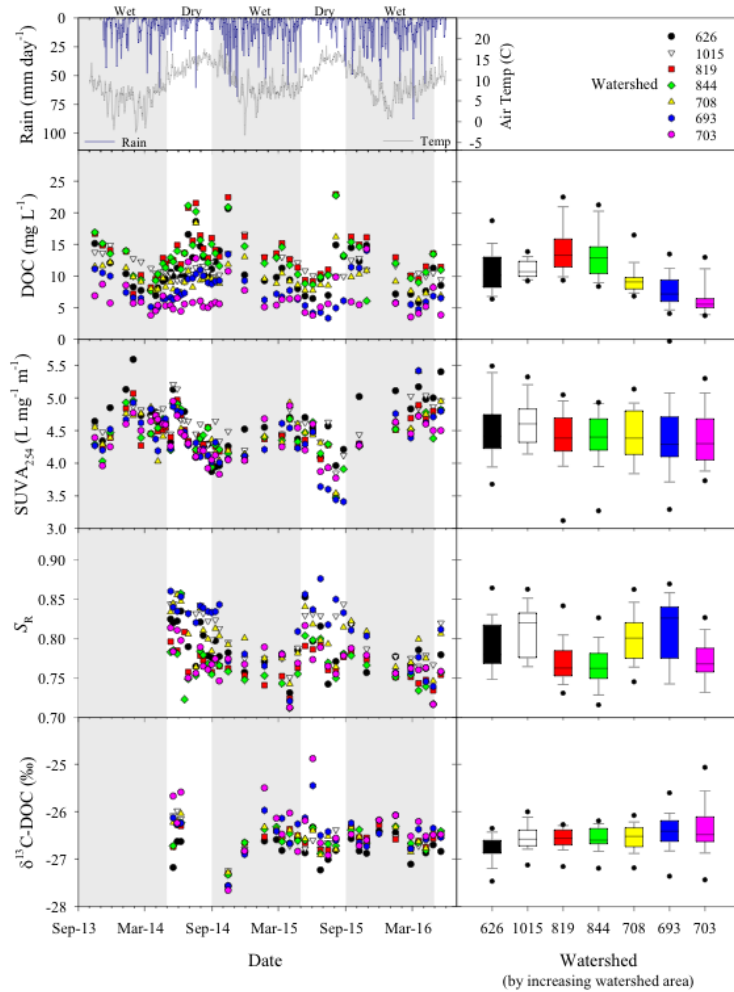
1208
1209
1210
1211
1212
1213
1214
1215
1216
1217
1218
1219
1220
1221
1222
1223
1224
1225
1226
1227
1228
1229
1230

1231 **Figure 2.** Hydrological patterns typical of watersheds located in the study area (a) the
 1232 hydrograph and precipitation record from Watershed 708 for the study period of October 1,
 1233 2015-April 30, 2016. Grey shading indicates the wet period (September 1-April 30) and the
 1234 unshaded region indicates the dry period (May 1-August 30) (b) Correlation of daily (24 hour)
 1235 areal runoff (discharge of all watersheds combined) to 48 hour total rainfall recorded at
 1236 watershed 708. For the period of study, comparisons of daily runoff to 48-hr rainfall
 1237 (runoff:rainfall mean= 0.92, std \pm 0.27) indicated rapid discharge response to rainfall.
 1238



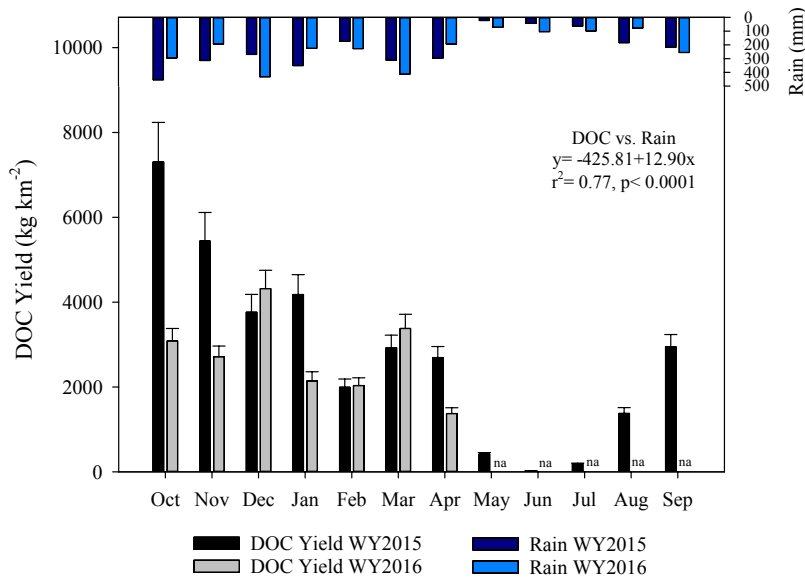
1239
 1240
 1241
 1242
 1243

1244 **Figure 3.** Seasonal (timelines, by date) and spatial (boxplots, by watershed) patterns in DOC
 1245 concentration and DOM composition for stream water collected at the outlets of the seven study
 1246 watersheds on Calvert and Hecate Islands. Boxes represent the 25th and 75th percentile, while
 1247 whiskers represent the 5th and 95th percentile. Daily precipitation and annual temperature are
 1248 shown in the top left panel. Grey shading indicates the wet period (September 1-April 30) and
 1249 the unshaded region indicates the dry period of each water year.



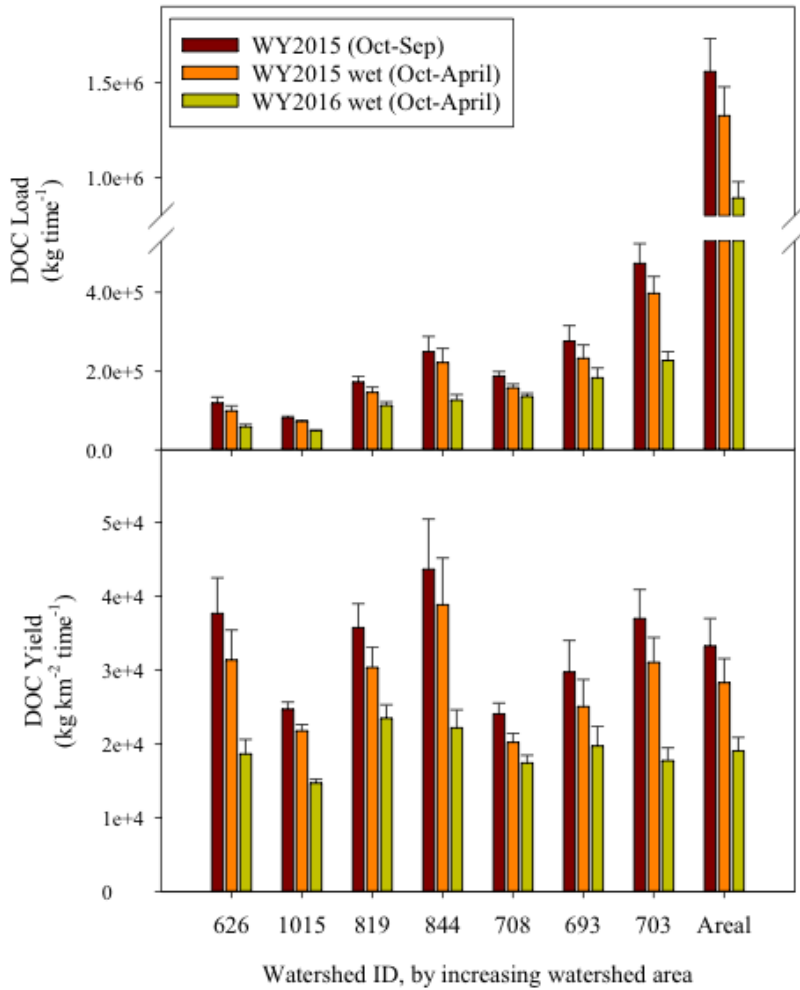
1250
 1251
 1252
 1253
 1254
 1255
 1256
 1257
 1258
 1259

1260 **Figure 4.** Monthly areal DOC yields and precipitation for water year 2015 (WY2015) and the
 1261 wet period (October 1-April 30) of water year 2016 (WY2016). Error bars represent standard
 1262 error. Total rain and DOC yield were significantly correlated ($r^2 = 0.77$) and months of higher
 1263 rain produced higher DOC yields. In WY2015, the majority of DOC export (~94% of annual
 1264 flux) occurred during the wet period (~88% of annual precipitation).

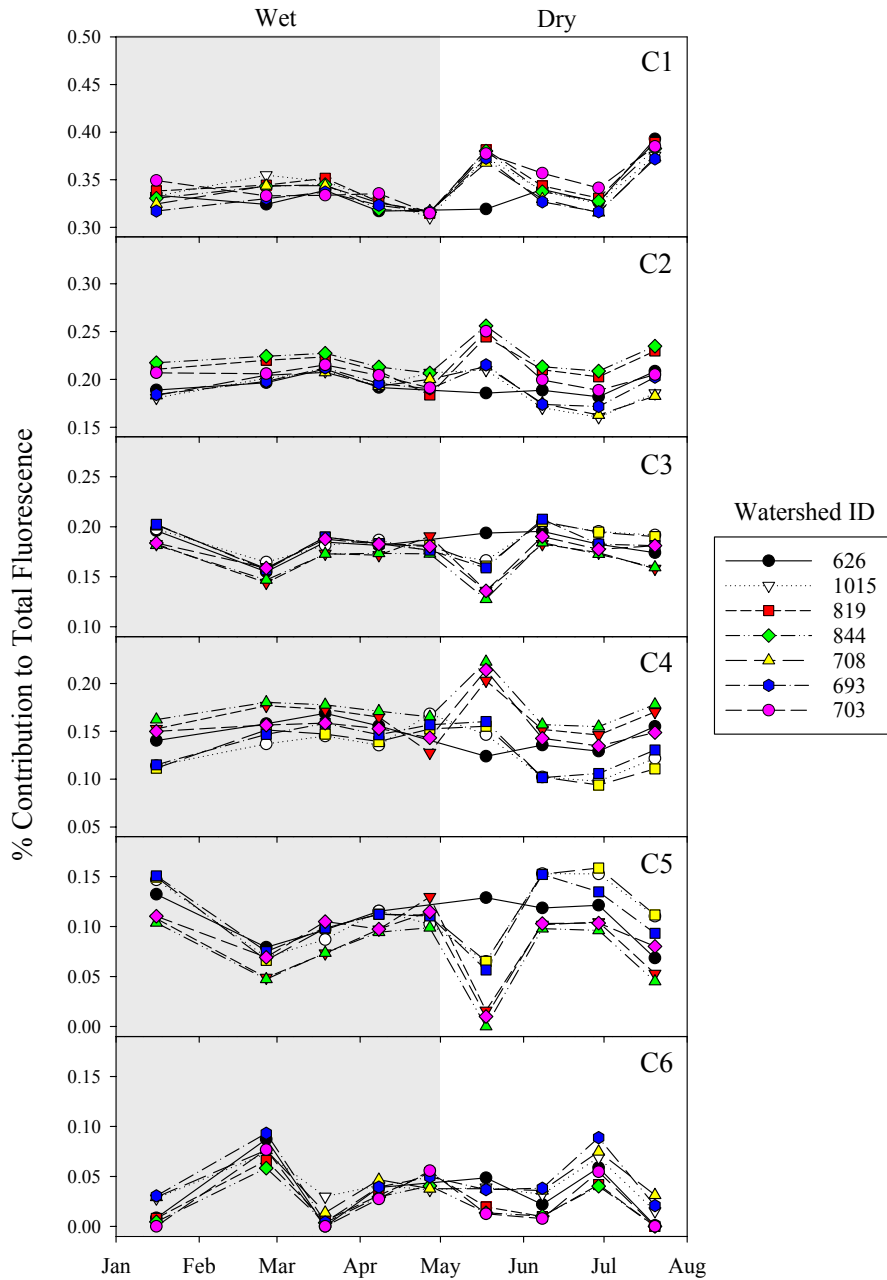


1265
 1266
 1267
 1268
 1269
 1270
 1271
 1272
 1273
 1274
 1275
 1276
 1277
 1278

1279 **Figure 5:** DOC fluxes and yields for the seven study watersheds and the total area of study
 1280 (“areal”, all watersheds combined) on Calvert and Hecate Islands for water year 2015 (WY2015;
 1281 Oct 1 - Sep 30), and October 1- April 30 of the wet period for water year 2015 (WY2015 wet)
 1282 and water year 2016 (WY2016 wet). Because DOC yields were only available for September in
 1283 WY2015, this month was excluded from the wet period totals in order to make similar
 1284 comparisons between years. Error bars represent standard error.

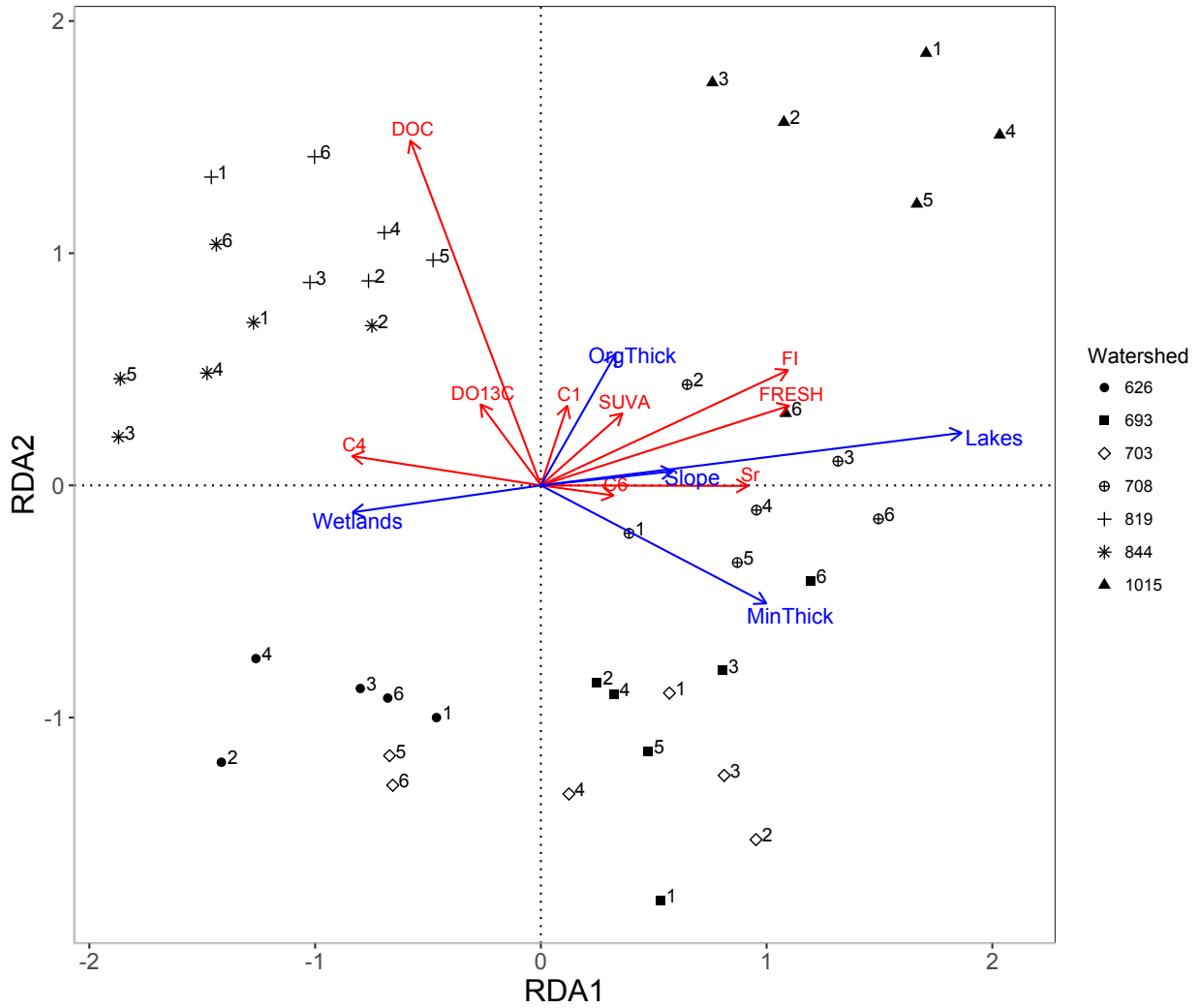


1286 **Figure 6:** Percent contribution of the six components identified in parallel factor analysis
 1287 (PARAFAC) for samples collected every three weeks from January-July, 2016 from the seven
 1288 study watersheds on Calvert and Hecate Islands. The grey shading indicates the wet period and
 1289 the unshaded region indicates the dry period. Note that while the y-axis for each panel has a
 1290 range of 20%, the max and min for each y-axis varies by panel.



1291
 1292

1293 **Figure 7:** Results from the partial-Redundancy analysis (RDA; type 2 scaling) of DOC
 1294 concentration and DOM composition versus watershed characteristics. Angles between vectors
 1295 represent correlation, i.e., smaller angles indicate higher correlation. Symbols represent different
 1296 watersheds, and numbers on symbols represent the sample month in 2016: 1= January, 2=
 1297 February, 3= March, 4= early April, 5= late April, and 6= May.
 1298



1299

1300 **Table 1:** Watershed characteristics, discharge, DOC concentrations, and DOC yields for the seven study watersheds on Calvert and
 1301 Hecate Islands. Additional details on the methods used to determine watershed characteristics can be found in Supplemental Material.
 1302

Watershed	Area (km ²)	Avg. Slope (%)	Lakes (% Area)	Wetlands (% Area)	Avg. Depth Organic Soils (cm)	Avg. Depth Mineral Soils (cm)	Total Q Yield* (mm)	DOC* ^a (mg L ⁻¹)	Q-weighted Avg. DOC* (mg L ⁻¹)	DOC Annual Yield ^b WY2015* (Mg C km ⁻²)	DOC Monthly Yield ^b Wet Season** (Mg C km ⁻²)	DOC Monthly Yield ^b Dry Season*** (Mg C km ⁻²)
626	3.2	21.7	4.7	48.0	39.4 ±24.3	30.8 ±8.3	3673	11.0 ±3.5	15.3	37.7 (31.9 – 44.2)	3.59 (3.05 – 4.18)	0.62 (0.49 – 0.77)
1015	3.3	34.2	9.1	23.8	39.5 ±17.2	33.7 ±8.6	3052	11.2 ±1.6	12.9	24.7 (23.6 – 25.8)	2.56 (2.45 – 2.78)	0.27 (0.25 – 0.28)
819	4.8	30.1	0.3	50.2	37.9 ±19.1	29.8 ±5.7	3066	14.0 ±3.5	19.3	35.7 (31.7 – 40.2)	3.80 (3.37 – 5.10)	0.57 (0.48 – 0.67)
844	5.7	32.5	0.3	35.2	35.4 ±18.0	29.1 ±6.4	4129	13.1 ±3.6	15.9	43.6 (34.2 – 54.9)	4.24 (3.36 – 5.30)	0.54 (0.36 – 0.77)
708	7.8	28.5	7.5	46.3	36.2 ±19.7	29.9 ±6.0	3805	9.5 ±2.4	10.9	24.1 (22.2 – 26.0)	2.67 (2.46 – 4.07)	0.38 (0.34 – 0.43)
693	9.3	30.2	4.4	42.8	35.4 ±16.1	30.2 ±6.4	5866	7.7 ±2.5	8.4	29.7 (25.9 – 34.0)	3.19 (2.79 – 4.94)	0.41 (0.32 – 0.52)
703	12.8	40.3	1.9	24.3	37.3 ±16.5	35.8 ±13.4	6058	6.3 ±2.6	9.0	37.0 (32.5 – 42.0)	3.48 (3.07 – 4.02)	0.64 (0.52 – 0.77)
All	46.9	32.7	3.7	37.1	37.4 ±17.7	32.2 ±9.2	4730	10.4 ±3.8	11.1	33.3 (28.9 – 38.1)	3.35 (2.94 – 4.40)	0.50 (0.41 – 0.62)

* Calculated for water year 2015 (WY2015; Oct 1, 2014-Sep 30, 2015)

** Wet period average monthly yield calculated from October-April and September, WY2015 and October-April, WY2016

*** Dry period average monthly yield calculated from May-August, WY2015

^a Mean ± standard deviation

^b Total ± 95% confidence interval

1303 **Table 2:** Spectral composition for the six fluorescence components identified using PARAFAC, including excitation (Ex.) and
 1304 emission (Em.) peak values, percent composition across all samples, and likely structure and characteristics of the fluorescent
 1305 component based on previous studies.
 1306

Component	Ex. (nm)	Em. (nm)	% Composition ^a	Potential structure/Characteristics	Previous studies with comparable results
C1	315	436	34.1 ±2.2 (31.1-39.3)	Humic-like, less processed terrestrial, high molecular weight, widespread but highest in wetland and forest environment	Garcia et al. 2015(C1); Graeber et al. 2012(C1); Walker et al. 2014(C1); Yamashita et al. 2011(C1); Cory & McKnight, 2005(C1)
C2	270/ 380	484	20.2 ±1.9 (16.1-25.6)	Humic-like, resembles fulvic acid, widespread, high molecular weight terrestrial	Stedmon and Markager, 2005(C2); Stedmon et al. 2003(C3); Cory & McKnight, 2005(C5)
C3	270	478	17.8 ±1.8 (12.8-20.8)	Humic-like, highly processed terrestrial; suggested as refractory	Stedmon & Markager, 2005(C1); Yamashita et al. 2010(C2)
C4	305/ 435	522	14.8 ±2.6 (9.4-22.3)	Not commonly reported, similarities to fulvic-like, contributed from soils	Lochmuller & Saavedra, 1986(E)
C5	325	442	9.8 ±3.5 (0.0-15.9)	Aquatic humic-like from terrestrial environments; autochthonous, microbial produced; may be photoproducted	Boehme & Coble, 2000(Peak C); Coble et al. 1998(Peak C); Stedmon et al., 2003(C3)
C6	285	338	3.4 ±2.5 (0.0-9.3)	Amino acid-like/Tryptophan-like. Freshly added from land, autochthonous. Rapidly photodegradable	Murphy et al. 2008(C7); Shutova et al. 2003(C4); Stedmon et al. 2007(C7); Yamashita et al. 2003(C5)

^a Mean ± stdev (min-max) from all samples